Science and Technology for Energy Transition **77**, 15 (2022)

https://doi.org/10.2516/stet/2022011

Available online at:
stet-review.org

REGULAR ARTICLE OPEN ACCESS

The industrial-grade hemp (*Cannabis sativa* L.) seed oil biodiesel application in a diesel engine: combustion, harmful pollutants, and performance characteristics

Zeki Yilbaşi[1,*], Murat Kadir Yesilyurt[2,*], Hayri Yaman[3], and Mevlut Arslan[2]

[1] Department of Automotive Technology, Yozgat Vocational School, Yozgat Bozok University, 66200 Yozgat, Turkey
[2] Department of Mechanical Engineering, Faculty of Engineering-Architecture, Yozgat Bozok University, 66200 Yozgat, Turkey
[3] Department of Automotive Technology, Kırıkkale Vocational School, Kırıkkale University, 71450 Kırıkkale, Turkey

Received: 2 August 2021 / Accepted: 5 April 2022

Abstract. The core focus of the present investigation is regarding biodiesel production from industrial hemp seed oil applying single-stage homogenous catalyzed transesterification process obtaining high yield of methyl ester. The engine tests were carried out on a single-cylinder, four-stroke, water-cooled, unmodified diesel engine operating with hemp seed oil methyl ester as well as its blends with conventional diesel fuel. The experimental findings of the test fuels were compared with those from diesel. The results pointed out that the performance and combustion behaviors of biodiesel fuels are just about in line with those of diesel fuel propensity. The specific fuel consumption for 5% biodiesel blend (0.291 kg/kW h), 10% biodiesel blend (0.305 kg/kW h), and 20% biodiesel blend (0.312 kg/kW h) blends at full load was closer to diesel (0.275 kg/kW h). In the meantime, the thermal efficiency for biodiesel was found to be at the range of 15.98–24.97% and it was slightly lower than that of diesel (18.10–29.85%) at the working loads. On the other hand, the harmful pollutant characteristics of carbon monoxide, hydrocarbon, and smoke opacity for biodiesel and its blends were observed to be lower in comparison with diesel during the trials. However, the oxides of nitrogen emissions for biodiesel were monitored to be as 6.85–15.40 g/kW h which was remarkably higher than that of diesel (4.71–8.63 g/kW h). Besides that, the combustion behaviors of biodiesel and its blends with diesel showed much the same followed those of diesel. Namely, the duration of ignition delay of biodiesel–diesel blends was shorter than that of diesel fuel because of the higher cetane number specification of the methyl ester. The highest gas pressures inside the cylinder as well as the rates of the heat release of biodiesel including test fuels are lower in contrast to the diesel due to the shorter ignition delay. It could be concluded that the utilization of biodiesel produced from industrial hemp seed oil in the diesel engine up to 20% (by vol.) will decrease the consumption of diesel and environmental pollution, especially in developing countries.

Key words: Industrial-grade hemp, Biodiesel, Engine performance, Exhaust emissions, Combustion behaviors.

Nomenclature

BSFC	Brake Specific Fuel Consumption
BSEC	Brake Specific Energy Consumption
B100	100% biodiesel
B10	90% diesel fuel + 10% biodiesel (by vol.)
EGT	Exhaust Gas Temperature
CO_2	Carbon dioxide
UHC	Unburned Hydrocarbon
CP	In-cylinder gas pressure
CP_{max}	Maximum in-cylinder gas pressure
$AHRR_{max}$	Angle of maximum Heat Release Rate
KOH	Potassium Hydroxide
RSM	Response Surface Methodology
GA	Genetic Algorithm
θ	Crank angle
P	Pressure of the cylinder
CHR	Cumulative Heat Release
$ACHR_{max}$	Angle of maximum Cumulative Heat Release
MFB	Mass Fraction Burned
m	Adjustable parameter
Δθ	Total combustion duration
EOC	End of Combustion

* Corresponding authors: zeki.yilbasi@bozok.edu.tr; kadir.yesilyurt@bozok.edu.tr

SOI	Start of the Injection process
$\left(\frac{dP}{dt}\right)_{max}$,	
PRR_{max}	Maximum Pressure Rise Rate
AIP_{max}	Angle of maximum Increase Pressure
R	Gas constant
N	Engine speed
F	Force
$\dot{m}_f$	Mass flow rate of the fuel
T_i	Mean gas temperature
V_i	Cylinder volume
P_{ref}	Reference pressure
w_R	Uncertainty degree of the results
$x_1, x_2, \ldots, x_n$	Independent variables
θ_{CS}	Crank angle where the combustion starts
RIN	Ringing Intensity
$AMGT_{max}$	Angle of maximum Mean Gas Temperature
BP	Brake Power
BTE	Brake Thermal Efficiency
B5	95% diesel fuel + 5% biodiesel (by vol.)
B20	80% diesel fuel + 20% biodiesel (by vol.)
NO_X	Oxides of nitrogen
CO	Carbon monoxide
O_2	Oxygen
ACP_{max}	Angle of maximum in-cylinder gas pressure
HRR	Rate of the Heat Release
HRR_{max}	Maximum Rate of Heat Release
NaOH	Sodium hydroxide
ANN	Artificial Neural Network
Q_{net}	Amount of energy
γ	Constant polytrophic exponent
V	Volume of the cylinder
CHR_{max}	Maximum Cumulative Heat Release
FLP_{max}	Fuel Line Pressure
a	Adjustable parameter
θ_0	Beginning of the combustion
SOC	Start of Combustion
IDP	Ignition Delay Period
PRR	Pressure Rise Rate
P_{max}	Maximum cylinder gas pressure
T_{max}	Maximum gas temperature in the cylinder
β	Correlation constant
T	Brake torque
Q	Energy supplied from the fuel
LHV	Lower Heating Value
P_i	Pressure
T_{ref}	Reference temperature
V_{ref}	Reference volume
θ_{IN}	Crank angle where the fuel injects
$w_1, w_2, \ldots, w_n$	Uncertainty values for the independent variables
R	Dependent factor related to the independent variables
MGT	Mean Gas Temperature
MGT_{max}	Maximum Mean Gas Temperature

1 Introduction

In the course of the date, energy has been one of the most basic necessities as a means to keep going any activity in casual life [1]. However, energy usage and demand all over the world have been swiftly expanding caused by modernization, industrialization, growing population, and enhancements in the living standards of humans from the time of the 21st century [2–4]. Contrary to the year 2016, the consumption of primary energy in the world rose by 2.2% in 2017. Correspondingly, fossil-based fuels have been the most predominant energy resource in terms of the rate of 85% [5]. That rate has not varied in the last century and is predicted that it could not change for a more few decades [6]. The present resources of fossil-based fuels like petroleum and coal have been diminishing rapidly. Unfortunately, the available reserves of fossil-based fuels are finite since they are not renewable energy resources. In this regard, it is forecasted that fossil-based fuel reserves will be totally exhausted in near future [7–9].

Internal combustion engines (especially compression-ignition engines) have performed a considerable role in most sectors such as agriculture, transportation, power generation, etc. [10, 11]. Because of environmental issues, high cost, and permanent expenditure of petroleum-based non-renewable fuels, the requisition for renewable, and sustainable fuel resources has come into view. In another word, the aforementioned annoyances have quickened the shifting to alternating energy sources that can be employed in place of petroleum-based fuels [12–14]. For that reason, some attempts have been made to decline the elevated dependency on fossil-based fuels all over the world in recent years. In conclusion, the scientific society has embarked upon searching for developed and alternative energy resources that might help to bring down global warming worldwide and to overcome the environmental pollution affairs [15, 16].

Biodiesel is an alternative fuel for diesel engine applications synthesized from the reaction of vegetable oils, animal fats, waste cooking oils, algae oils, etc. [17, 18] in the existence of a catalyst (homogenous, heterogeneous, and enzymes) with alcohol (generally lower-order alcohol) such as ethanol or methanol [19, 20]. Biodiesel is non-toxic, biodegradable, and free of sulfur [21]. Additionally, it is an environmentally friendly fuel because it can release fewer emissions compared to those arising from the burning of fossil-based fuels [22–24]. On one hand, the oxygen content of their chemical structures is approximately 10–11% [25], on the other hand, the cetane numbers are between 49 and 62 in general [26]. With the assistance of the surplus amount of oxygen in their chemical bonds, they happen to improve the oxygen concentration of the fuel blend by mixing with diesel fuel and hence enhance the combustion quality [27–29].

The performance of the engine has exceedingly pertained to the qualification of the sprayed fuel into the cylinder, the formation of the atomization and vaporization, fuel/air ratio in the combustion chamber, and the characteristics (viscosity, density, etc.) of the used fuel [30]. A collection of properties like energy content, cetane number, etc. are also mightily interconnected with the fuel density. As is well-known, the viscosity and density of the fuel influence the injection characteristics, and therefore, they happen a great effect on the combustion behaviors, engine performance, and emission profiles [31]. Indeed, the regular utilization of biodiesel fuels in many countries can reduce subjection to the fuels provided from petroleum bought from other countries, especially where the countries do not have reserves. Therefore, these countries would be less influenced by the sudden cost variation resulting in a probable oil crisis that can happen in the next term. In addition, this situation includes the back demand to affect the countries' economies positively [3, 32].

For the above-mentioned grounds, biodiesel fuels have lots of advantages and great potency in respect of alternative fuels both in the present and future. On top of this, the disposition to biodiesel is an encouraging technique to descend the fuel reliance of the countries. The non-edible raw materials involve the *Pongamia pinnata* [33], *Jatropha curcas* [33], *Calophyllum inophyllum* [34], *Brucea javanica* [35], *Madhuca indica* [36], *Raphnus raphanistrum* [37], *Brassica juncea* [38], *Styrax officinalis* [39], *Sinapis alba* [40], *Brassica nigra* [41], *Hevea brasiliensis* [42] and *Crambe abyssinica* [43] have been used as a remarkable fuel source for the synthesis of biodiesel in the recent literature. In this context, industrial hemp (*Cannabis sativa* L.) seed oil can be subjected to be one of the most significant non-edible raw materials in the production of biodiesel for Turkey. It is to be highlighted that a limited number of researches carried out regarding the hemp seed oil methyl ester and its blends with diesel fuel in the current literature [44–46]. Li *et al.* [47] produced biodiesel from industrial hemp seed oil *via* base-catalyzed transesterification reaction. The yield of the product was observed to be at 97% while the ester conversion rate was found to be 99.5%. The researchers implemented several tests for determining the quality of the derived biodiesel, including flash point, kinematic viscosity, acid number, sulfur content, etc. the pronounced characteristics of the hemp seed oil biodiesel was kinematic viscosity (3.48 mm^2/s) and cloud point (−5 °C). As a consequence, hemp seed oil biodiesel became competitive and engaging due to the above-stated properties. A distinct study was carried out by Gupta and co-workers [48] who developed a solar energy-assisted transesterification process using Fresnel lens solar concentrator and compared the results with the conventional heating approach for hemp seed oil biodiesel production considering various process parameters. The researchers monitored that the maximum biodiesel yield was achieved as 97.37% using Fresnel lens solar concentrator at catalyst amount of 0.9 wt.%, alcohol to oil molar ratio of 4.5:1, stirring speed of 200 rpm, and temperature of 60 °C. In the meantime, the highest product yield of 21.3% using the conventional heating approach was observed at the aforementioned optimized reaction conditions. Stamenković *et al.* [49] optimized the reaction variables of the transesterification process using methanol in the presence of KOH by the Response Surface Methodology (RSM) and Artificial Neural Network model along with the Genetic Algorithm (ANN-GA). Consequently, the highest biodiesel yield was estimated to be 99.8% applying the RSM model while 99.8% using the ANN-GA model. Ravichandra *et al.* [50] investigated the biodiesel derived from Deccan hemp seed oil and its blends aiming to run on the diesel engine. The experimental findings demonstrated that the BTE was enhanced by 4.15% by using B50 in comparison with the conventional diesel fuel. The emission results showed that the biodiesel decreased UHC, CO, and NO_X while increasing the carbon dioxide (CO_2) and smoke opacities with the rise in the biodiesel percentage in the fuel blend. The Ignition Delay Period (IDP) and duration of the combustion were observed longer with using biodiesel in contrast to the diesel fuel's entire loading conditions. Jayaraman *et al.* [51] studied the influence of hydrogen infusion into the Deccan hemp seed oil and its biodiesel product on the emissions, performance, and combustion characteristics of a compression-ignition engine operated at part load and full load conditions with a constant speed of 1500 rpm. The researchers found that the BTE values were increased from 27.3 to 29.6% and 29.7 to 32.6% under a full loading condition of the tested engine powered by hydrogen doped biodiesel and virgin vegetable oil. UHC, CO, and smoke opacity emissions descended for all test fuels about the unmodified diesel fuel while an increase in the NO_X emissions was monitored because hydrogen addition led to high rates of combustion and high temperature inside the cylinder. Ahmad *et al.* [44] analyzed the physical and chemical properties of produced hemp seed oil biodiesel at the optimized reaction conditions. The conversion yield of the oil to the biodiesel was detected to be 75.90% under the methanol to oil molar ratio of 6:1, reaction temperature of 60 °C, and using potassium hydroxide (KOH) concentration of 0.67%. The fuel properties of hemp seed oil biodiesel met within the range of the ASTM D6751. John and Raja [45] investigated the exhaust emissions (CO, HC, NO_X, smoke), engine performance (thermal efficiency, specific fuel consumption, mechanical efficiency), and combustion behaviors (cylinder pressure, heat release rate) of a diesel engine fueled with hemp seed oil biodiesel blends (10, 20, 30, 40, and 50%). The findings indicated the industrial hemp seed oil biodiesel could be used as a raw material in the production of biodiesel and also B30 gave the optimal outcomes based on the combustion, performance, and exhaust emission attributes. Mohammed *et al.* [46] measured some properties such as TGA, DSC, UV–Vis, and FT–IR of hemp seed oil biodiesel blends with diesel, diethyl ether, and butanol to discuss the characteristics with standards. As observed from discussed literature above, just about limited parameters, especially in combustion characteristics, were examined and the researchers did not use pure biodiesel in the engine. It is, therefore, investigated systemically the influences of the engine performance, combustion behaviors, and exhaust emission levels by doping hemp seed oil methyl ester into the mineral diesel fuel in the present paper. In addition, the results were compared

with the other studies. In this way, this work supports that the suitability of the hemp seed oil methyl ester and its blends as a nature-friendly alternate fuel for CI engines. Due to the limited number of studies, it is recommended that related studies shall be further investigated.

2 Industrial hemp (*Cannabis sativa* L.)

Cannabis (commonly known as hemp) belongs to the family of the Cannabaceae and its scientific name is "*Cannabis sativa* L." [45]. The systematic position of hemp is given as follows: "Kingdom – Plantae (Plants), Subkingdom – Tracheobionta (Vascular plants), Superdivision – Spermatophyta (Seed plants), Division – Magnoliophyta (Flowering plants), Class – Magnoliopsida (Dicotyledons), Subclass – Hamamelididae, Order – Urticales, Family – Cannabaceae (Hemp family), Genus – Cannabis L., Species – *Cannabis sativa* L." [52]. The hemp plant picture was demonstrated in the Supplementary data file (Fig. 1S) in Section A.

Hemp is a kind of herbaceous plant and the usage of this plant leans in its oilseed, industrial-grade fiber, medicine, recreation, and food [53, 54]. It is stated that the native hemp plant, an annual crop, is in Western and Central Asia. In addition, hemp can be seen in Sub-Himalayan regions of India. It has been grown in wasteland places [45]. As is well-known, hemp has been utilized as a raw material in the textile industry for centuries. Moreover, it has been pointed out that hemp could be used in various sectors like automotive, paper, high-quality absorbents, personal cleaning, plastics, agriculture, medicine, paints carpets, insulation, household goods, varnish, and construction materials [55]. However, the extractions of narcotics, crude oil, and fiber are the particular objectives in the production of these plants. In recent years, non-edible oil extracted from industrial-grade hemp seeds commenced having great importance for countries. On the other hand, the above-mentioned literature survey indicated that a few works were performed with the goal of biodiesel production from hemp seed oil. Measuring the physical and chemical characteristics for assessing the attributes of the hemp seed oil biodiesel has been investigated and it has been highlighted that the free fatty acid number of the hemp seed oil was found to be lower than 2% [44]. Since hemp seed has 26–38% oil content, it has been taken into consideration as an eventual raw material for the production of biodiesel. Besides that, its fiber has 20–30% carbohydrates, 20–25% protein, 10–15% insoluble fiber, and rich content of minerals [45].

Although hemp seed oil has a non-edible characteristic, there is no commercial biodiesel production from this oil all over the world to the best of the authors' knowledge. Nevertheless, hemp seeds have been consumed after being roasted (called "kavurga" in Turkey) by people in Anatolia for a long time [56]. Due to the above-reported stronger reasons, hemp seed oil can be evaluated as a promising feedstock in the production of biodiesel. Considerable physicochemical properties of hemp seed oil biodiesel such as kinematic viscosity, calorific value, density, specific gravity, flash point, fire point, cold flow properties, etc. have been addressed. They resemble most of the other biodiesel fuels synthesized from different vegetable oils. Therefore, this paper concentrates on the derivation of biodiesel from crude oil extracted from hemp seeds thanks to a cold press apparatus and examines systematically the performance, exhaust emissions, and combustion characteristics of a compression-ignition engine fueled with hemp seed oil biodiesel and its blends with conventional diesel fuel at different percentages. In this context, this study is a pioneer in this field.

3 The scope of the study

On the reports of the surveyed literature studies, previously conducted works have been mostly performed to monitor the optimization of the reaction conditions in the biodiesel production and to determine the physicochemical specifications of the hemp seed oil methyl ester. On the other hand, it can be observed that the researches performed with hemp seed oil methyl ester in the reviewed literature are contemplated to detect the engine characteristics and combustion behaviors at various engine operating conditions. For the aforementioned reasons, it has believed by the authors that this article has stateliness as a means to deliver a direction to future studies on the combustion characteristics, emission profiles, and engine performance parameters of blending hemp seed oil methyl ester into the mineral diesel fuel. In addition to this, industrial hemp has strategic significance since it has started to be supported by the government. The core objective of the present study is to establish experimentally the effects on the neat hemp seed oil methyl ester and its blends with conventional diesel fuel about the engine performance, combustion behaviors, and harmful pollutant features at various engine loading conditions (25%, 50%, 75%, and 100% corresponding to 8.35, 16.70, 24.82, and 33.39 Nm, respectively) for various biodiesel–diesel fuel blends (B5, B10, B20, and B100) and reference fuel (diesel fuel).

4 Materials and experimental procedures

4.1 Materials and reagents

The seeds of the industrial-grade hemp plant used in this experimental research were purchased from a commercial local market located in Konya, Turkey. The distribution of the hemp plant growing places in the world and the regions allowed by the government for cultivating hemp plants in Turkey are shown in the Supplementary data file (Fig. 2S) in Section A.

The chemicals and reagents employed in the present experimental study were selected on basis of convenience and ease of attainment. To produce biodiesel, the transesterification technique was selected in this study because this method is more dependable and advantageous on account of its low cost, short reaction duration, direct conversion process, need low pressure and temperature, and gives high

(a) *(b)* *(c)*

Fig. 1. The steps belonging to the extraction of the hemp seed unrefined oil (a: Hemp seeds, b: Oil extraction stage, and c: Filtered oil).

product yield [57]. In the transesterification process, methanol (lower-order alcohol that purity of 99.9%) was chosen as alcohol, and KOH (purity of higher than 90%) was selected as an alkali catalyst because of its reaction activity. Alcohol was procured from *Merck Chemical Company* (Darmstadt, Germany) and KOH pellet was supplied from *Tekkim Chemical Company* (Bursa, Turkey). The qualitative filter paper (125 mm) was used for the filtration of biodiesel and crude oil after the cold pressing process was bought from *S&H Labware* (Ankara, Turkey). For measuring the free fatty acid content (oleic %) and acid number (mg/KOHg) of the samples, KOH solution (0.1N) and phenolphthalein indicator (1%) were purchased from *Norateks Chemical Company* (Istanbul, Turkey), diethyl ether (purity of $>$ 99.5%) was taken from *Isolab* (Wertheim, Germany), and ethanol (purity of $>$ 99.5%) was purchased from *Sigma-Aldrich Chemical Company* (St. Louis, Missouri, USA). The reference standards of the fatty acid methyl esters (purity of $>$ 99%) were also bought from *Sigma-Aldrich Chemical Company* (St. Louis, Missouri, USA). The whole reagents used in the experimental stages were employed as received forms, namely so as not to implement any more purification stages on the grounds of their analytical class. In the stage of the washing process of the biodiesel, the distilled water was obtained thanks to a convenient apparatus (the Millipore brand Direct-Q 8UV model). Besides that, other kinds of equipment such as spoons, magnetic stirrer bars, glassware, etc. used in the trials were ensured from a regional market that has EN ISO 17025 accreditation and ISO 9001 Quality Management certificates.

4.2 Experimental procedures

4.2.1 The extraction of crude oil from industrial grade hemp seeds

The procured seeds of the hemp plant shown in Figure 1a were cleaned from impurities manually. Afterward, the seeds were dried under the sunlight for one week to decrease the moisture content. A screw press machine was used for obtaining the hemp seed crude oil demonstrated in Figure 1b. The hemp seed crude oil was put in a sealed glass container and rested for three weeks to subside the oil cake particles with the help of the gravity impact and density difference. After waiting, the upper part of the oil phase was poured out of an identical container and then the coarse filtering process was carried out to this crude oil in a view to remove the suspended oil cake particles with the aid of cloth material. Afterward, the fine filtering process was applied to the crude oil using a qualitative filter paper. In conclusion, filtered and clean oil was employed in the production stage of biodiesel. The obtained hemp seed crude oil was illustrated in Figure 1c. However, the alternating fuel preferred as an engine fuel must be inexpensive and eco-friendly [58]. The above-reported problem can be solved by converting this unrefined oil into biodiesel fuel at which its specifications and performance are almost similar to those of conventional diesel fuel [59].

The physical and chemical characterizations of the hemp seed crude oil used in the production of methyl ester were presented in Table 1. In addition to this, the aforesaid properties compared with those of different vegetable-based oils preferred frequently in the production of biodiesel were also summarized in the same table. Details have been shown in Table 1 that give out the fuel properties of hemp seed crude oil as nearly in line with other raw materials referred to in the recent literature. As observed, the oils originating from vegetables have higher kinematic viscosity, lower energy content, and higher density. For that reason, the utilization of neat vegetable oils in the compression-ignition engines has led to the occurrence of several difficulties such as the formation of gum, engine choking, piston sticking, and clogging of the fuel injector. In conclusion, it can be easily stated that vegetable oils are not appropriate alternating fuels for compression-ignition engines for long-term applications due to the above-mentioned problems [60].

4.2.2 The production of hemp seed oil methyl ester

It is well-known that transesterification is the process of replacing the organic R group of an ester with the organic R group of an alcohol. That reaction is usually catalyzed by the induction of a base or acid catalyst. The mechanism

Table 1. The physical and chemical characterizations of hemp seed crude oil and their comparison with other vegetable oils used in the production of biodiesel.

Property	Unit	Hemp seed oil	Hemp seed oil [46]	Hemp seed oil [47]	*Styrax officinalis* seed oil [39]	Safflower oil [61]	Juliflora seed oil [62]	Linseed oil [63]	Palm oil [60]	Honne oil [64]	Rubber seed oil [65]
Density at 15 °C	kg/m^3	0.930	927.9	918	909 (at 20 °C)	921.03	930 (at 40 °C)	924	913	910	910
Kinematic viscosity at 40 °C	mm^2/s	26.95	27.28	26.46	–	32.102	37.784	16.23	40.55	32.48	76.4
Flash point	°C	>150	–	232	228	229	181	108	290	224	198
Acid value	mg KOH/g	3.5	3.857	0.67	3.88	–	–	–	–	4.76	53
FFA content	oleic %	1.75	–	–	1.94	–	4	–	–	2.38	–
Gross calorific value	MJ/kg	38.50	–	–	38.652	40.468	37.6	39.75	39.22	–	–
Cetane number	–	–	–	–	–	–	–	35	46	–	–
Pour point	°C	–	−22	–	–	−6	–	−5	–	–	–
Water content	ppm	<500	–	–	–	–	–	–	–	–	–

of the transesterification reaction is illustrated in the Supplementary data file (Fig. 3S) in Section A.

The entity of moisture in the oil used for biodiesel production may cause adverse impacts on the rate of the methyl ester conversion [66]. For that reason, there is a need to implement a pre-heating process for the oil to be used in the transesterification reaction. In this study, the pre-heating process was performed above 100 °C to eliminate the moisture content in the hemp seed crude oil. Then, the free fatty acid content of the hemp seed oil was measured to decide the number of stages in the transesterification reaction using an acid-base titration method. Due to having lower than 2% free fatty acid content, the hemp seed oil was directly converted to the methyl ester without the need for any pre-improvement stage. If the fatty acid concentration was higher than the limit value [67], the two-step transesterification method (acid transesterification reaction followed by the alkali transesterification reaction) will be performed to obtain methyl ester. Since the fatty acid content of hemp seed oil is below 2%, the extra cost and time are also saved.

The base-catalyzed transesterification reaction was conducted directly to the hemp seed oil because of the above-mentioned reasons. In the present work, the methyl ester synthesis from hemp seed oil was effectuated in the Biofuel Laboratory of the Department of Mechanical Engineering of *Yozgat Bozok University* (Turkey). To obtain the methyl ester from the oil, a small-scale laboratory-type biodiesel production reactor was used. This reactor has composed of a three-necked and flat bottom flask mounted with a reflux condenser on account of preventing the vaporization of the alcohol throughout the reaction. The prepared reactor was put down on the magnetic stirrer with a hot plate (*Scilogex* brand MS7-H550-Pro model), and there is a condensation system and sampling outlet. In the reaction, KOH was selected as a base catalyst with the object of mitigating the unsaturated fatty acids in the biodiesel. The alkali transesterification process was performed several times at various reaction parameters because of achieving the maximum conversion rate. The transesterification reaction of vegetable oils has been affected by dissimilar variables such as catalyst loading, nature of the catalyst, the temperature of the reaction, alcohol type, and its molar ratio to the oil. Experimental duration also plays a considerable role in acquiring methyl ester with the needed purity [59]. Most of the parameters which were indicated above were investigated for optimizing the methyl ester production process. As a consequence, the production of methyl ester from hemp seed oil was realized under the optimized reaction conditions. However, the temperature of the reaction was considered as below 64.7 °C because of the boiling point of the selected alcohol. The comprehensive biodiesel production stages were explained in the next paragraph for a better understanding of this process.

In the first place, 0.75 wt.% of KOH was dissolved in the alcohol (methanol) for 20 min at room temperature to avoid the alcohol's evaporation. After preparing the experimental apparatus, the hemp seed oil was discharged into the reactor for a single-step transesterification reaction. When the temperature of the oil reached the wanted reaction temperature, the prepared methoxide solution was put into the biodiesel reactor to commence the reaction. During the reaction, the agitation intensity was kept constant at 500 rpm. In the aftermath of the transesterification reaction, the mixture was poured into a separation funnel without waiting and settled a minimum of 8 h for subsiding the glycerol phase. Figure 4S (a) in the Supplementary data file Section A shows a photographic sight of the phase separation. Following this, the precipitated phase was taken with the aid of a drainage valve, and the resultant upper phase was discharged in a similar flask. Then, the temperature of the product was increased up to the boiling point of the alcohol to remove the excessive amount of alcohol that has been found in the biodiesel. Directly after, the product was again poured into the separation funnel and waited to descend the temperature to 55 °C. The washing process was implemented to the product at the same temperature as the distilled water. An image captured right after the washing

process was also shown in Figure 4S (b) in the Supplementary data file Section A. The washed methyl ester was rested for approximately 12 h to sink the wastewater, next it was heated above 120 °C by 2 h to remove the surplus water by courtesy of evaporation in the biodiesel. In the end, waiting for the temperature of the fuel to drop and the final product was stored for further studies and recognition in a glass bottle at a medium that does not see light.

The production stages from the hemp seed to the methyl ester were briefly illustrated as in the flowchart given in Figure 2.

4.2.3 Preparation of tested fuel samples

The synthesized hemp seed oil methyl ester was blended with commercially available mineral diesel fuel with particular concentrations to acquire the test fuel samples that were projected to be employed in the experimental step of the current research. Fundamentally, neat hemp seed oil methyl ester and its three different proportions into the diesel fuel were experienced in the tests. The produced methyl ester was doped into the conventional diesel fuel at the proportions of 5%, 10%, and 20% on a volume basis applying splash blending technique with the help of a calibrated beaker having an accuracy of ± 0.5 mL to ensure the precise blending ratios. Besides that, the trials were also performed using conventional diesel fuel in order how to influence methyl ester on the engine performance, harmful pollutants, and combustion behaviors. The abbreviations of the biodiesel–diesel fuel blends were denominated to be at DxBy in which D and B have referred to the name of the diesel fuel and biodiesel, respectively while x and y have ascribed to the proportions of diesel fuel and biodiesel of total volume, respectively. For the simplicity of the presentment and understanding in this work, however, D was deleted, and just By presentation was used. In this regard, the abbreviations of the test fuel samples that were used in this study and their blending concentrations were tabulated in Table 1S in the Supplementary data file Section B.

The entire test fuel specimens one after another have been constituted and warehoused in different sealed glass containers at the dark place under the laboratory climates for two weeks on account of monitoring whether the phase segregation issues are or not. Following the storage period, the authors have not seen any phase separation in the fuel mixtures. Each respective prepared test fuel sample was more than adequate convenient at the laboratory conditions. Before the engine tests, on the other hand, each specific fuel sample was shuffled in the fuel tank to remove any possible phase separation in terms of prevention errors and faults. A photographic appearance of hemp seed oil methyl ester, conventional diesel fuel, and their binary blends (B5, B10, and B20) has been shown in Figure 5S in the Supplementary data file Section A. Table 2 presents some of the significant physical and chemical characteristics of the test fuel samples.

4.2.4 Engine test set-up

In the present experimental study, the engine parameters including performance, harmful pollutants, and combustion behaviors for the obtained test fuel samples (biodiesel and its blends with conventional diesel fuel) were experienced on the engine test set-up located in Automotive Laboratory, Department of Automotive Technology, *Kırıkkale Vocational School, Kırıkkale University*, Kırıkkale, Turkey. The engine experiments were carried out on a four-stroke, single-cylinder, water-cooled, naturally-aspirated, direct-injection, multi-fuel research engine fabricated by *Apex Innovations Pvt. Ltd.* in India. The stroke and bore of the tested engine were 110 mm and 87.50 mm, respectively. The detailed engine specifications were displayed in Table 2S in the Supplementary data file Section B.

An AC (Active Current) dynamometer with air-cooled (*Galen-Tech brand*) having a loading unit was connected to the crankshaft of the researched engine and operated for loading the engine to change the engine loads with increments of 25% from 0 to 100%. By the way, *Siemens* make the Sinamics G120 PM250 power module with regenerative type constant speed was used as a dynamometer loading unit. A fixed engine speed of 1500 rpm was supplied for each fuel type during the experiment. The fuel consumption of the engine was measured by recording the volume deciphered for 60 s with the aid of an assembly standard burette. For noting the fuel consumption duration, a standard stopwatch was employed. The measurement of the airflow rate taken into the engine cylinder was determined using a standard air tank framework including a manometer and an orifice meter apparatus. To measure the temperatures from different parts of the engine, K-type thermocouples were mounted on suitable locations. In this study, the combustion characteristics of the engine running on the prepared test fuel samples at various engine loading

Fig. 2. Flowchart of biodiesel production stages from hemp seed in this work.

Table 2. Some of the significant physical and chemical characteristics of the test fuel samples.

Property	Unit	Diesel fuel	B100
Chemical formula	–	$C_{14}H_{25}$	$C_{17.60}H_{30.47}O_2$
Density at 15 °C	kg/m^3	823.1[a]	875
Cetane number	–	53.5[*,a]	36.498
Kinematic viscosity at 40 °C	mm^2/s	2.645	3.429
Calorific value	kJ/kg	43850	38737
Carbon	wt.%	87.05	77.18
Hydrogen	wt.%	12.95	11.13
Oxygen	wt.%	–	11.69
Carbon/Hydrogen	–	6.722	6.934
Flash point	°C	59[a]	>120
Water content	ppm	80[a]	<500
Copper strip corrosion (3 h at 50 °C)	Degree of corrosion	1A	1A
pH	–	7.0	6.5
Ash content	% (m/m)	0.01	0.01
Group I metals (Na + K)	mg/kg	–	133.1
Group II metals (Ca + Mg)	mg/kg	–	16.23
Total contamination	mg/kg	<12[a]	–
Acid value	mg KOH/g	0.2	0.4
Linolenic acid methyl ester	% (m/m)	–	17.84
Polyunsaturated (≥4 double bonds) methyl esters	% (m/m)	–	0
Saponification value	mg KOH/g	–	200.616
Iodine value	g I_2/100 g	–	164.482
Cloud point	°C	−8	−1.56
Cold filter plugging point	°C	−25[a]	−7.08
Pour point	°C	−35	−8.52
Oxidation stability	hour	–	9.757
P content	mg/kg	–	90.17
Mn content	mg/kg	–	0.08
Distillation – 250 °C	% (v/v)	47.2[a]	–
Distillation – 350 °C	% (v/v)	93.9[a]	–
Distillation – 95% recovered at °C	°C	355[a]	–
Sulfur	mg/kg	5.6[a]	–

[*] Cetane index.
[a] These values were adopted from the supplier.

conditions were also analyzed comprehensively. In this context, a pressure sensor (*PCB Piezotronics* brand S111A22 model) is diaphragm stainless steel type and hermetic sealed. The measurement range of the aforesaid transducer is 5000 psi with a sensitivity of 1.0 mV/psi. Also, a low noise cable was used to avoid the environmental noise effect on the signals. A crank angle encoder (*Kubler* make 8. KIS40.1361.0360 model) with a TDC pulse was placed to measure the position of the crankshaft and the resolution of the encoder is provided from the supplier as 1 deg. The acquired cylinder gas pressure and crank angle coming from the tests for each fuel type at various engine loads were recorded to decipher the rate of the heat release and other combustion parameters such as ignition delay period, mass fraction burnt, etc. with the help of a *National Instrument* make NI USB-6210 bus-powered M series multifunction data acquisition device. Supplementary data files about the details of the engine instrumentations which were used in the present work (Table 3S) were tabulated in Section B.

The exhaust emission profiles of the biodiesel and its blends with mineral diesel fuel on the engine such as Carbon Monoxide (CO), Unburned Hydrocarbon (UHC), Oxygen (O_2), Carbon Dioxide (CO_2), and Oxides of Nitrogen (NO_X) were recorded thanks to a *Bilsa* brand MOD 2210 model (five gas analyzer). The smoke opacity measurements were performed by using a *Bosch* brand BEA 350 model having RTM 430 model smoke meter kit. The technical specifications of the exhaust emissions measurement device and smoke opacity meter were given in Table 4S in Section B of the Supplementary data file.

In conclusion, software-originated engine performance appraisals have been taken into consideration, and thence

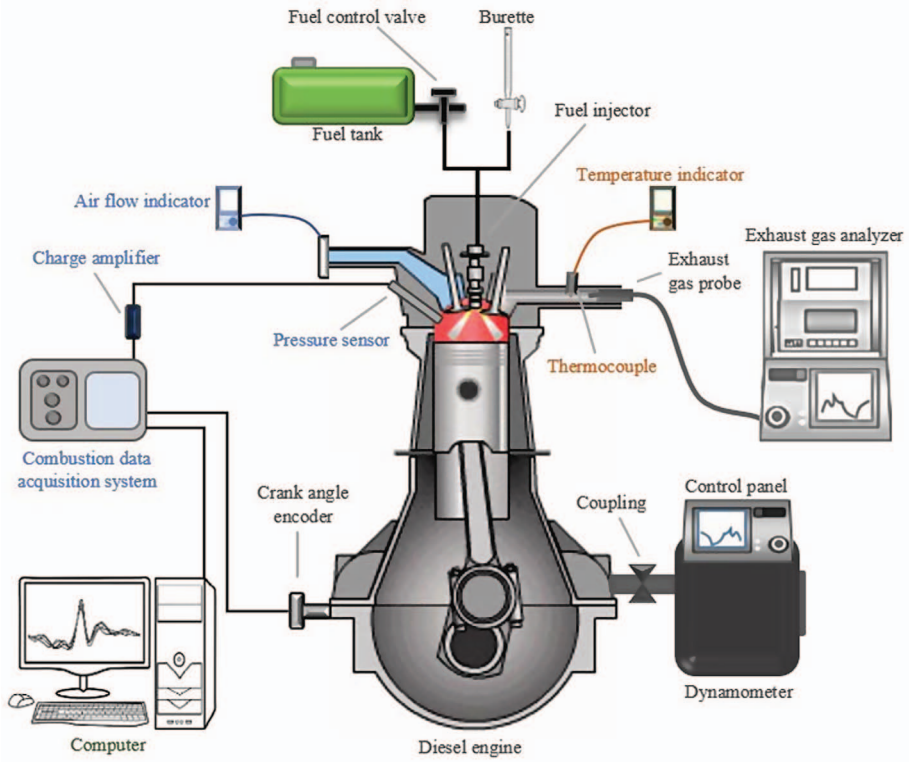

Fig. 3. A schematic diagram of the test engine and related pieces of equipment layout.

the outcomes have been constituted coming from the analyses. The achieved data with regards to the experimental research have been laid up for further assessments of the engine performance, combustion characteristics, and harmful pollutant profiles of the aforesaid tested fuel specimens. The exhaust gases were, on the other hand, immediately released to the atmosphere *via* a stainless steel pipe without any dilution technique. A schematic diagram of the researched engine and related pieces of equipment was displayed in Figure 3 and a photographic view of the test setup was exhibited in Figure 6S in Section A of the Supplementary data file.

4.2.5 Methodology of the engine tests

Preliminary to commencing the researched engine, the levels of fuel and lubricating oil were checked out intending to guarantee they were in the appropriate levels. Then, to facilitate the experiments, the engine was operated with conventional diesel fuel aiming to warm up the engine for 30 min. The temperature of the cooling water has come to 60 °C in the aftermath of the warm-up duration where engine trials for various engine loads were changed by selecting the convenient load with the help of an active current dynamometer in the steps of 3.7 kg from 3.7 kg to 14.9 kg which was corresponding to 25% from 25% to 100%. The engine speed and wanted brake power generation were kept constant for each situation by the governor of the engine. In an attempt to enhance the reliability of the findings obtained from the experimental tests, the rate of fuel consumption was detected thanks to a stopwatch and standard burette equipment. In this way, the engine performance and exhaust emission tests were conducted. The engine cooling water flow rate was kept fixed to be 250 L/h during the experiments. These experiments were repeated three times and subsequently; the average values of the outcomes were taken into account in this work. Afterward, the engine operating indicators, *i.e.*, brake power (P_e), Brake Thermal Efficiency (BTE), Brake Specific Fuel Consumption (BSFC), and Brake Specific Energy Consumption (BSEC) with regards to the engine loads were determined and noted down for each fuel type. After obtaining the experimental data in the trials, some of the engine performance values were determined with the help of using equations (1)–(6) represented underneath [68, 69]:

$$P_e = \frac{2\pi NT}{60 \cdot 1000}, \tag{1}$$

$$T = F \cdot 0.230, \tag{2}$$

$$\mathrm{BTE} = \frac{P_e}{Q}, \tag{3}$$

$$Q = \dot{m}_\mathrm{f} \cdot \mathrm{LHV}, \tag{4}$$

$$\mathrm{BSFC} = \frac{\dot{m}_\mathrm{f}}{P_e}, \tag{5}$$

$$\mathrm{BSEC} = \frac{\dot{m}_\mathrm{f} \cdot \mathrm{LHV}}{P_e}, \tag{6}$$

where N shows the engine speed, T indicates the engine torque, F is the force, Q demonstrates the energy supplied from the tested fuel, $\dot{m}_f$ is the mass flow rate of the tested fuel, and LHV is the lower heating value of the fuel.

Exhaust Gas Temperature (EGT) was also measured and compared with each other. Additionally, exhaust gas emissions, namely, UHC, CO_2, CO, O_2, NO_X, and smoke opacity values were monitored using an exhaust gas analyzer device and smoke opacity meter. Before starting the measurement of the harmful pollutants, the devices were calibrated using reference gases to figure out the righteousness of the recorded data. In addition, the smoke opacity measurement device was arranged to its zero point before measurement. All of the experimentations referring to the assessment of the characteristics were carried out in steady-state conditions of the engine.

As soon as the preliminary experimentations were over, the fundamental tests were executed using hemp seed oil biodiesel and its blends with conventional diesel fuel to evaluate the performance, combustion, and emission characteristics of the diesel engine after all deficiencies were removed. For entire the trials, the engine was commenced firstly with mineral diesel fuel and put up with stabilizing for 30 min. Succeeding the tested engine was warmed up, the test fuels (B5, B10, B20, and B100) were filled out to the fuel tank. The engine characteristics of low percentage biodiesel–diesel fuel mixtures such as B5 and B10 displayed an almost identical trend to baseline diesel fuel on account of facilitating proportion on higher blend percentages for the experimentations. Achieving the end of the test, the fuel tank was discharged and then, filled with diesel fuel. Next, the engine was re-operated for a while to scrub off the tested fuels from the injection system as well as the fuel lines, and then, it was closed. Through this, it helped prevent cold start problems to some extent. Throughout the experimentations, the relative humidity and the ambient temperature were observed to be 55–60% and 19–21 °C, respectively. The unmodified mineral diesel fuel has been used as a reference fuel to acquire comparative results.

The gas pressure outcomes inside the cylinder of the researched compression-ignition engine have been noted down for each engine working cycle from beginning to 720° crank angle in each one-degree crank angle step at all of the engine loading conditions as above mentioned. Furthermore, the mean cylinder gas pressure values for entire test fuel samples have been considered after applying an appropriate filtering technique accounting for at least 50 engine cycles. "ICEngineSoft" which is a Lab view-based engine performance analysis software packaged program was employed to obtain and evaluate the performance and combustion results.

The augmentation of the internal energy during the combustion process occurring in the cylinder and the rate of the Heat Release (HRR) figures that convert to the mechanical net-work agreeing with the crank angle have been estimated taking into consideration equation (7) based on the 1st law of thermodynamics [70]:

$$\frac{\mathrm{d}Q_{\mathrm{net}}}{\mathrm{d}\theta} = \frac{\gamma}{\gamma-1} P \frac{\mathrm{d}V}{\mathrm{d}\theta} + \frac{1}{\gamma-1} V \frac{\mathrm{d}P}{\mathrm{d}\theta}, \tag{7}$$

where Q_{net} refers to the amount of energy, θ shows the crank angle, γ indicates the constant polytrophic exponent, P is the cylinder gas pressure, and lastly, V is the volume of the cylinder. In the calculation of the HRR values, the heat losses from the cylinder wall were not taken into consideration. By the way, γ was kept constant during the analyses to be 1.35.

The Cumulative Heat Release (CHR) can be identified as the integral of heat release over a limited crank angle gap. The CHR results for each type of tested fuel were calculated considering equation (8), as given underneath [71]:

$$Q_{\mathrm{cum}} = \int Q_{\mathrm{net}} = \int P \frac{\gamma}{\gamma-1} \frac{\mathrm{d}V}{\mathrm{d}\theta} + V \frac{1}{\gamma-1} \frac{\mathrm{d}P}{\mathrm{d}\theta}, \tag{8}$$

where Q_{cum} demonstrates the cumulative heat release.

In this study, the rate of the Pressure Rise (PRR) was found considering a numerical derivative method applied to the filtered pressure data coming from the analyses. The Mass Fraction Burned (MFB) values were also taken into consideration for an expressive combustion evaluation in terms of a better understanding of the subject. The MFB is a key parameter for dissimilar combustion process phases that take place in a compression-ignition engine concerning the crank angle position. In different words, the MFB can be described as the aggregated released heat output in sequential crank angles at the intervals of commencing and finishing of the combustion process by overall heat released in the total duration of the combustion. The MFB values with regards to the crank angle for each tested fuel sample were computed using the following formula [72]:

$$\mathrm{MFB} = 1 - \exp\left[-a\left(\frac{\theta-\theta_0}{\Delta\theta}\right)^{m+1}\right], \tag{9}$$

where a and m indicate the adjustable parameters, θ_0 shows the beginning of the combustion, and $\Delta\theta$ refers to the total combustion duration.

The other remarkable combustion parameters were also taken into account for each fuel type at various engine loading conditions. The Start of the Combustion (SOC) and the End of the Combustion (EOC) were obtained to be kept in view the 5% and 90% of the total heat release, respectively. The interval from SOC to EOC was considered to be the duration of the combustion process (CD). The Start of the Injection (SOI) process can be described as the crank angle where the fuel injector arrives at the nozzle opening pressure which was monitored to be approximately 200 bar. The Ignition Delay Period (IDP) is determined to be the difference between the SOI and SOC. To find the IDP, most of the researchers have recommended the following formula [73–75]:

$$\mathrm{IDP} = \theta_{\mathrm{CS}} - \theta_{\mathrm{IN}}, \tag{10}$$

where θ_{CS} is the crank angle where the combustion commences and it is acquired from the $\frac{\mathrm{d}P}{\mathrm{d}\theta}$ curve as it varies its shape when the burning was occurred. θ_{IN} is the standard fuel injection timing and it was taken from the specifications of the supplier. In this study, the standard fuel injection timing was applied to be 23° before TDC.

In this work, to evaluate the trend of the knock for the researched compression-ignition engine [76], the Ringing Intensity (RIN), also named as the ringing index, for each tested fuel sample at different engine loads was estimated using the following formula which was recommended by Soloiu *et al.* [77, 78]. RIN has been taken into consideration for the DI compression-ignition engine by Wei *et al.* [79] even though this index has been completely implemented as the basic indicator to monitor the knock inclination for the homogenous charge compression-ignition engines. It is highlighted that the considerable advantage of the RIN formula has been reported that it can be appraised on account of measuring the knock in the simulation of the tested engine with ease because such models suggested by researchers cannot give high-frequency oscillations [80]:

$$\mathrm{RIN} = \frac{1}{2\gamma}\frac{\left[\beta\left(\frac{\mathrm{d}P}{\mathrm{d}t}\right)_{\max}\right]^2}{P_{\max}}\sqrt{\gamma R T_{\max}} \tag{11}$$

in its equation, $\left(\frac{\mathrm{d}P}{\mathrm{d}t}\right)_{\max}$ shows the maximum PRR, $P_{\max}$ refers to the maximum cylinder gas pressure occurred inside the cylinder, $T_{\max}$ demonstrates the maximum gas temperature in the engine cylinder. R and β are a gas constant and a correlation constant, respectively. A correlation constant is generally taken to be as 0.05 ms [80] even though it can be changed according to the engine geometry.

In addition, the mean gas temperature is calculated from equation (12) derived from the ideal gas law [81]:

$$T_i = P_i V_i \frac{T_{\mathrm{ref}}}{P_{\mathrm{ref}} V_{\mathrm{ref}}}. \tag{12}$$

In the above-mentioned formula, T_i, P_i, and V_i show the mean gas temperature, pressure, and cylinder volume while T_{ref}, P_{ref}, and V_{ref} indicate the reference values at any point of the polytrophic curve of expansion.

4.2.6 Error analysis

It is to be noticed that the overall uncertainty of the current scrutinizations has been examined by computing the accuracies for the dissimilar measuring pieces of equipment connected to the engine set-up. The repeatability for the measurements was observed to be reasonably dissimilar. This case can be because of the observation, reading, environmental conditions, standardization, quality of the apparatus, sequence of tests, irregularities, and so on. Based on the uncertainty for the apparatus, the uncertainty analysis was carried out using the technique of distribution of the errors, as suggested by Holman [82]. The formula for estimating the uncertainties is shown below:

$$w_R = \left[\left(\frac{\partial R}{\partial x_1}w_1\right)^2 + \left(\frac{\partial R}{\partial x_2}w_2\right)^2 + \ldots + \left(\frac{\partial R}{\partial x_n}w_n\right)^2\right]^{12} \tag{13}$$

here, w_{R} points out the uncertainty degree of the results. R indicates a dependent factor and it is related to the independent variables. x_1, x_2, …, x_{n} are the independent variables meanwhile w_1, w_2, …, w_n are the corresponding uncertainty values.

The uncertainties of the measured and computed parameters based on equation (13) were displayed in Table 3.

The overall percentage uncertainty for the present experiment was found using the following formula [83–85]:

$$\begin{aligned}
&\text{The total uncertainty of the experiment performed in this study}\\
&= \text{square root of } \big((\text{uncertainty of pressure sensor})^2\\
&+ (\text{uncertainty of encoder})^2 + (\text{uncertainty of CO})^2\\
&+ (\text{uncertainty of } CO_2)^2 + (\text{uncertainty of UHC})^2\\
&+ (\text{uncertainty of } O_2)^2 + (\text{uncertainty of } NO_X)^2\\
&+ (\text{uncertainty of smoke opacity})^2\\
&+ (\text{uncertainty of temperature})^2\\
&+ (\text{uncertainty of burette system})^2\\
&+ (\text{uncertainty of stop watch})^2\\
&+ (\text{uncertainty of manometer})^2 + (\text{uncertainty of load})^2\\
&+ (\text{uncertainty of speed})^2)\\
&= \text{square root of } \big((0.53)^2\\
&+ (1.0)^2 + (0.75)^2 + (0.64)^2 + (0.98)^2 + (0.48)^2\\
&+ (0.92)^2 + (0.51)^2 + (0.72)^2 + (1.0)^2 + (0.2)^2\\
&+ (0.78)^2 + (0.83)^2 + (0.067)^2).
\end{aligned} \tag{14}$$

In conclusion, the total uncertainty for the performed experiment was acquired to ±2.722%.

5 Results and discussions

The combustion characteristics, harmful pollutants, and performance experiments were carried out on a single-cylinder, four-stroke, water-cooled, DI compression-ignition engine at a stable engine speed of 1500 rpm with various engine loading conditions (from 0 to 25% to full load at the steps of 25%) using hemp seed oil methyl ester and its blends with traditional diesel fuel (B5, B10, and B20). The outcomes obtained from the research such as BTE, BSFC, BSEC, EGT, CO, CO_2, O_2, NO_X, UHC, smoke opacity, cylinder gas pressure, HRR, CHR, PRR, MFB, IDP, and other combustion parameters for the above-stated tested fuel samples were systematically investigated in detail and compared with those from reference diesel fuel operation for better understanding the influence of alternating biodiesel fuels on the aforesaid engine characteristics.

5.1 Combustion and injection characteristics

In the following subsections, the injection and combustion behaviors of an unamended DI compression-ignition engine

Table 3. The uncertainties of the remarkable parameters.

Instrument			Percentage uncertainty (%)
Temperature indicator			± 0.72
Speed sensor			± 0.067
Pressure sensor			± 0.53
Fuel flow burette			± 1.00
Air flow rate			± 0.78
Time			± 0.20
Crank angle encoder			± 1.00
Load indicator			± 0.83
Engine power			± 0.72
Fuel consumption			± 0.48
Thermal efficiency			± 0.86
Exhaust gas analyzer	Range	Accuracy	
CO	0–10%	0.001%	± 0.75
CO_2	0–19.99%	0.001%	± 0.64
UHC	0–10000 ppm	1 ppm	± 0.98
O_2	0–25%	0.01%	± 0.48
NO_X	0–5000 ppm	1 ppm	± 0.92
Smoke intensity (k)	0–9.99 1/m	0.01 1/m	± 0.51

powered by hemp seed oil methyl ester, conventional diesel fuel, and its binary blends (B5, B10, and B20) have been observed under distinct engine loading conditions (from 25% to full load at the intervals of 25%) on account of understanding the mechanisms and processes of the combustion reactions takes place in the combustion chamber of the tested engine where the researched fuel specimens were combusted for constituting heat energy that depends up expressly on the physicochemical properties and intermolecular structures as well. In this context, cylinder gas pressure, the highest cylinder gas pressure, HRR, the peak HRR, CHR, PRR, IDP, RIN, and other remarkable combustion parameters have been meticulously addressed and discussed taking into account the findings surveyed in the present literature.

5.1.1 In-cylinder gas pressure

The in-cylinder gas pressure is a remarkable parameter that is imperative to investigate the characteristics of the combustion process in the combustion chamber, and further, for evaluating the engine performance. Figure 4 portrays the in-cylinder gas pressure results for hemp seed oil biodiesel and its blends with traditional diesel fuel according to the crank angle at the maximum engine loading condition. As is well-known, the physicochemical specifications of the fuels immensely influence the combustion behaviors of the compression-ignition engines. It is to be noted that the hemp seed oil biodiesel and its various binary blends with diesel fuel have followed up a close trend of diesel fuel operation at all working conditions. It can be recognized from Figure 4 that the peak in-cylinder gas pressure ascends with rising the engine load for each type of fuel since more fuel amount is sprayed into the combustion chamber and burned at higher loading conditions. To conclude, the highest in-cylinder gas pressure figures which were seen at the full load for baseline diesel fuel, B5, B10, B20, and B100 were found to be 85.44 bar, 83.42 bar, 83.04 bar, 82.72 bar, and 80.85 bar, respectively. As observed, diesel had the highest in-Cylinder Pressure (CP). In the meantime, hemp seed oil methyl ester reached a 4° after TDC where is the maximum gas pressure amongst the alternating fuel samples. It was approximately 5.68% lower than that of diesel operation mode at the maximum engine load. At higher engine loading conditions, temperature also augments in the matter of pressure, leading to a higher rate of evaporation and a preferable combustion process. This case was also explained by [86]. Chauhan *et al.* [87] pointed out that the earlier commencing of biodiesel-originated alternating fuel samples ignition and the peak in-cylinder gas pressure was monitored to be lower in comparison with the conventional diesel fuel. In addition, Qi *et al.* [88] reported that the maximum in-cylinder gas pressure was observed to be almost similar for all tested fuels. Asokan *et al.* [62] found that the highest in-cylinder gas pressure for juliflora oil biodiesel was 73.53 bar at the maximum engine load and it attained a 6° after TDC, while diesel had 73.91 bar.

5.1.2 Apparent heat release rate

The comparison of the apparent HRR values with regard to the crank angle for tested fuel samples at the highest engine loading condition was clearly illustrated in Figure 5. The net HRR curve helps to identify the quantity of heat energy that might be converted to beneficial work throughout the combustion process of the fuel. Similar to the in-cylinder pressure curves, the net HRR figures were increased

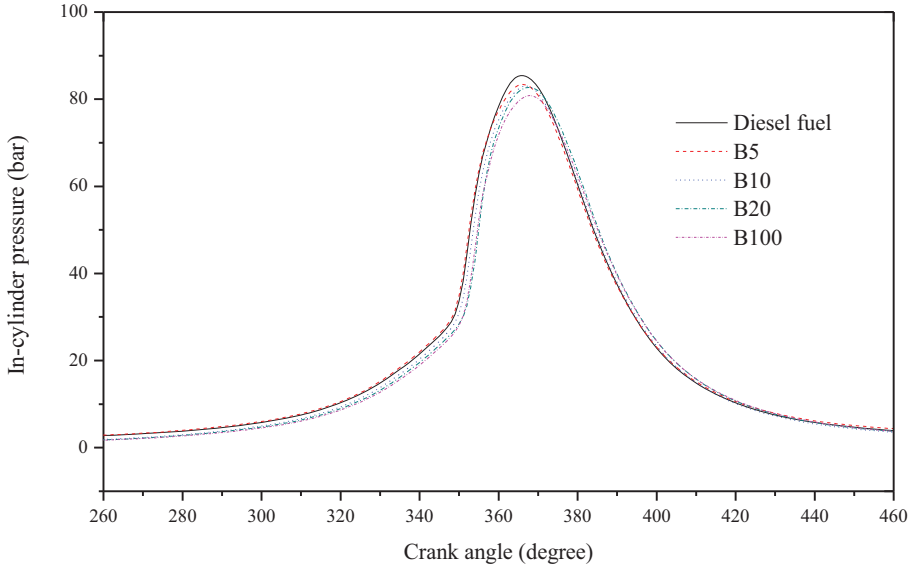

Fig. 4. The comparison of the in-cylinder gas pressure results with respect to the crank angle for each tested fuel at full load engine working condition.

with the augmentation of the engine load because of the aforementioned reasons. In this regard, the peak HRR values for traditional diesel fuel, B5, B10, B20, and B100 were calculated using the related formula to be 77.82 J/deg, 76.79 J/deg, 75.46 J/deg, 69.53 J/deg, and 66.73 J/deg, respectively. As predicted, the heat emitted during the diesel fuel operation was monitored to be higher than those of alternating biodiesel blends. Otherwise, the second-highest heat was released from the blend of B5. The B5 fuel blend and unmodified diesel fuel demonstrated a slight difference with a high rate of heat release in contrast to the other tested fuels. This can be addressed to be as the pressure is ascended considerably during the beginning phase of the combustion and the burning phase continued for a long time when the engine was fueled with biodiesel blends [62]. Besides that, the maximum apparent HRR figures for B5, B10, and B20 had nearly similar inclination with baseline diesel fuel under all engine loads whereas, the neat hemp seed oil biodiesel (B100) shows a progressive decrement in the maximum HRR. It is to be noted that pure biodiesel was 14.25% lower than that of traditional diesel fuel. This case is because of some important reasons. The lower apparent HRR of hemp seed oil biodiesel in comparison with the diesel fuel is owing to the shorter IDP and extended duration of the combustion process and also because of a lower heating value, high viscosity, and density specifications of the pure biodiesel. Additionally, biodiesel has a higher cetane rating than that of tested diesel fuel. The cetane number of the used fuel in the experimentations is fundamentally responsible for the process of the ignition [89] and for that reason, the SOC was observed to be a little bit earlier for biodiesel and its blends because their cetane numbers are slightly higher than that of traditional diesel fuel, as tabulated in Table 2. The shorter IDP leads to the accumulation of a lower amount of fuel at the stage of the pre-mixed combustion region. This brings about a decline in the highest HRR. In this framework, diesel fuel operation constitutes a longer pre-mixed combustion process which is accountable for a higher maximum in-cylinder gas pressure resulting in a higher PRR than hemp seed oil methyl ester. Chauhan *et al.* [87], for instance, indicated a higher maximum in-cylinder gas pressure meanwhile Qi *et al.* [88] showed the maximum net HRR for entire the tested fuel samples to be almost similar at low engine loading conditions, however, diesel fuel was slightly higher than those of biodiesel and its blends at high engine loads. Asokan *et al.* [58] highlighted that the net HRR of neat biodiesel was calculated to be low as compared to the diesel at higher engine loading conditions to worse spray behaviors and higher viscosity of biodiesel. To the top of this, the CHR curves, as given in the next subsection, have been plotted for better clearness and understanding of the aforesaid subject.

5.1.3 Cumulative Heat Release rate

Figure 6 plots the Cumulative Heat Release (CHR) concerning the crack angle at the engine load of 100% for traditional diesel fuel, hemp seed oil biodiesel, and their different binary blends. As observed, the maximum CHR values for diesel fuel, B5, B10, B20, and B100 were estimated to be 1.12 kJ, 1.0 kJ, 0.82 kJ, 0.78 kJ, and 0.76 kJ, respectively. The findings understandably point out that the maximal difference between diesel fuel and B100 is around 32%. On the other hand, diesel fuel released high CHR amongst the other biodiesel blends. The reason for this case can be explained as the poor transformation of heat energy to the crankshaft power in the mixture of biodiesel blends otherwise the conversion efficiency of the pure B100 fuel was monitored to be lower than those of other alternating tested fuel blends. This is presumably because of biodiesel's high density, low calorific value, high

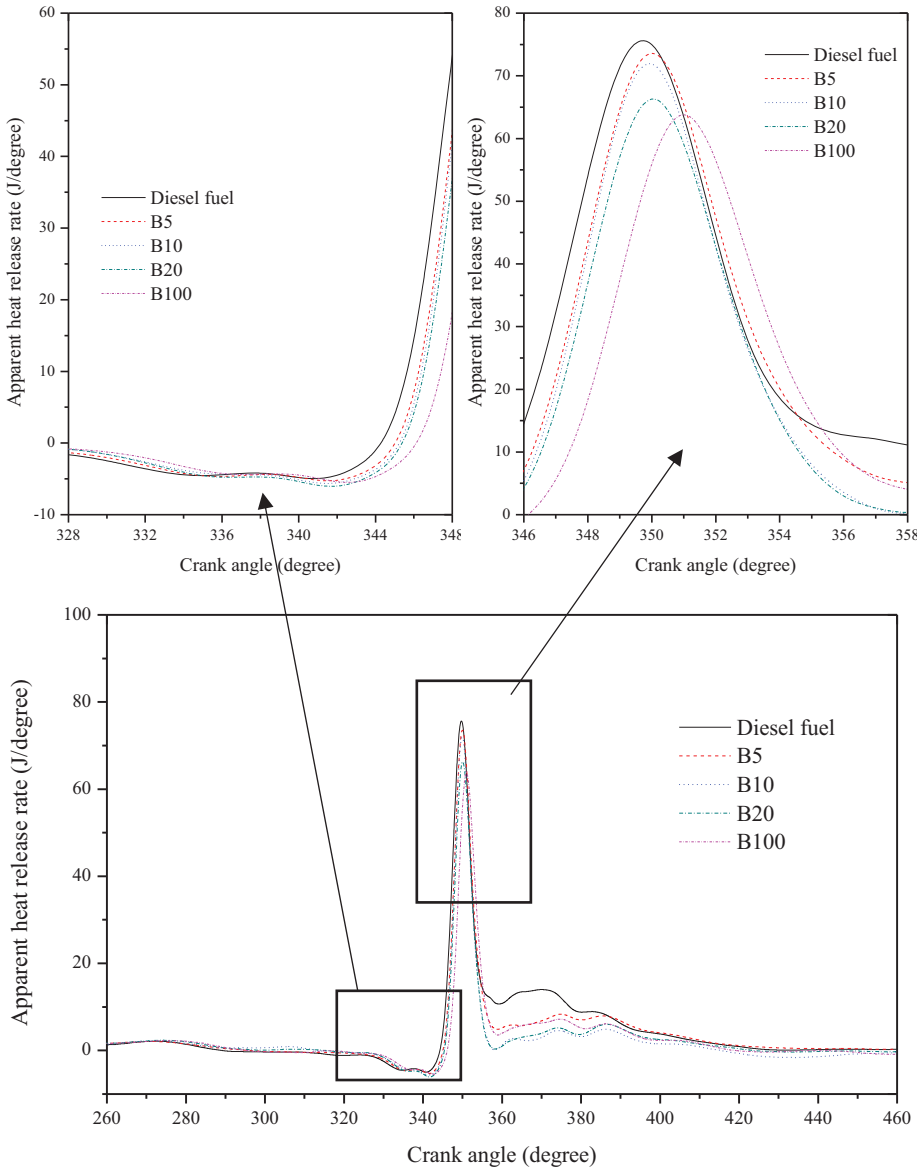

Fig. 5. The comparison of the apparent HRR results with respect to the crank angle for each tested fuel at full load engine working condition.

kinematic viscosity, and native oxygen molecules in its molecular structure. Similar arguments were also clarified by Asokan *et al.* [62] and Agarwal and Dhar [90].

5.1.4 Pressure Rise Rate

The variations of the pressure Rise Rate (PRR) curves for tested fuel samples with regards to the crank angle were shown in Figure 7. The maximum PRR has been taken into consideration to analyze the behavior of the knocking generation in the diesel engine. Moreover, the maximum PRR is used to establish the formation of NO_X emissions impended from the compression-ignition engines [91, 92]. It is to be noticed that the maximum PRR values ascended with the augmentation of the engine loads from 25% to 100%. In this context, at full load, the highest PRR was noted to be 6.2 bar/deg, 5.7 bar/deg, 6.1 bar/deg, 5.8 bar/deg, and 5.8 bar/deg for conventional diesel fuel, B100, B5, B10, and B20. In the case of the entire engine working conditions, the maximum PRR figures for pure biodiesel and its blends with diesel fuel declined than diesel fuel and were postponed further with besides rising concentrations of biodiesel in the tested fuel samples. In other words, diesel fuel operations led to a higher PRR than those of biodiesel blends at all engine loading conditions. The combustion process commenced earlier for biodiesel/diesel fuel blends owing to the shorter IDP, and for this reason, a few quantities of the mixtures were stayed at the end of the IDP, causing comparatively lower PRR [84, 93, 94]. It can be concluded that the usage of alternating biodiesel

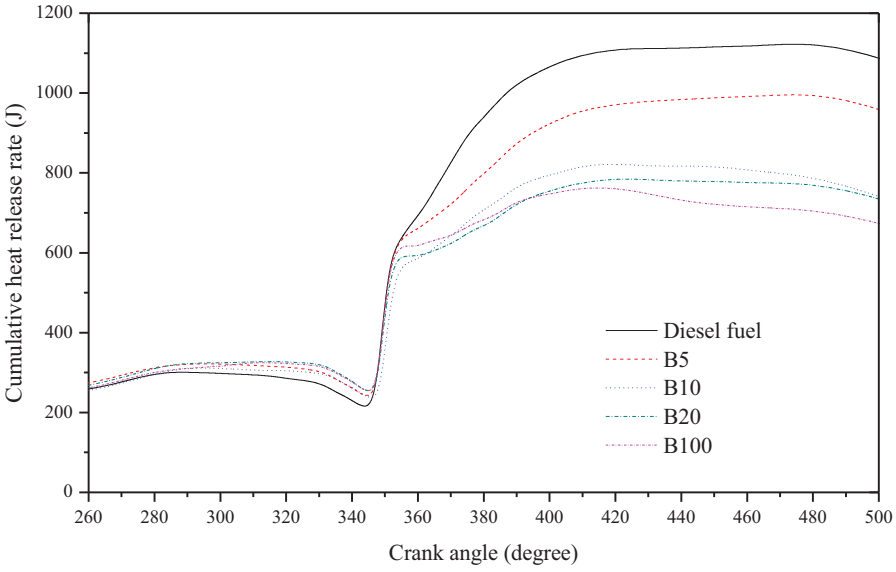

Fig. 6. The comparison of the CHR results with respect to the crank angle for each tested fuel at full load engine working condition.

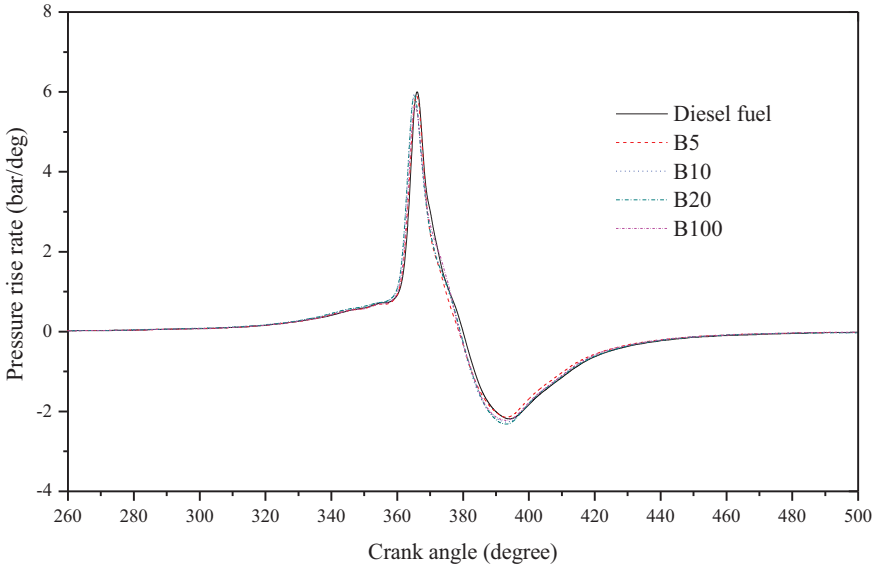

Fig. 7. The comparison of the PRR results with respect to the crank angle for each tested fuel at full load engine working condition.

blends is pervasive to the tendency of knocking in contrast to the mineral diesel fuel.

5.1.5 Ignition delay

One of the most significant parameters that affect the combustion process in the cylinder is the Ignition Delay Period (IDP). IDP can be identified as the ranging of the duration from the beginning of the fuel injected into the cylinder and the inception of the burning of fuel [84]. As known, it is a mandatory indicator employed on account of determining the ignition quality that has a straight affect on the delay of the ignition as well as the propensity to the knock for the used fuel. Figure 8 illustrates the alteration of the IDP according to the engine load for various test fuels. As reported earlier, a fuel having a higher cetane rating will bring about a shorter IDP and preferable diffusion phase process as compared to the pre-mixed combustion stage. That is to say, the cetane number of the fuel is inversely proportional to the IDP [95–97]. Commonly, biodiesel fuels and also their blends with diesel fuel possess higher cetane ratings in comparison to diesel fuel. However, the cetane number of the biodiesel synthesized from industrial-grade hemp seed oil was found to be lower than that of the

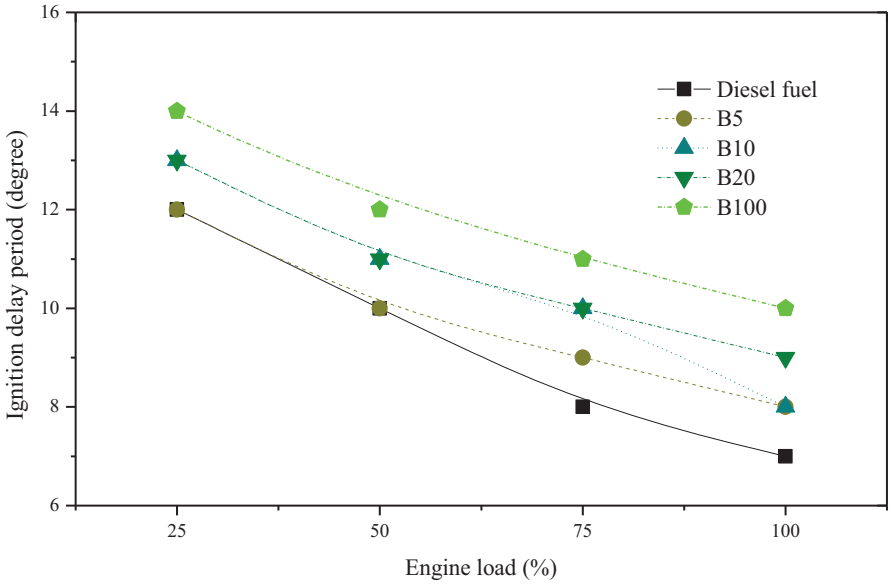

Fig. 8. The variation of IDP with respect to the engine load for tested fuels.

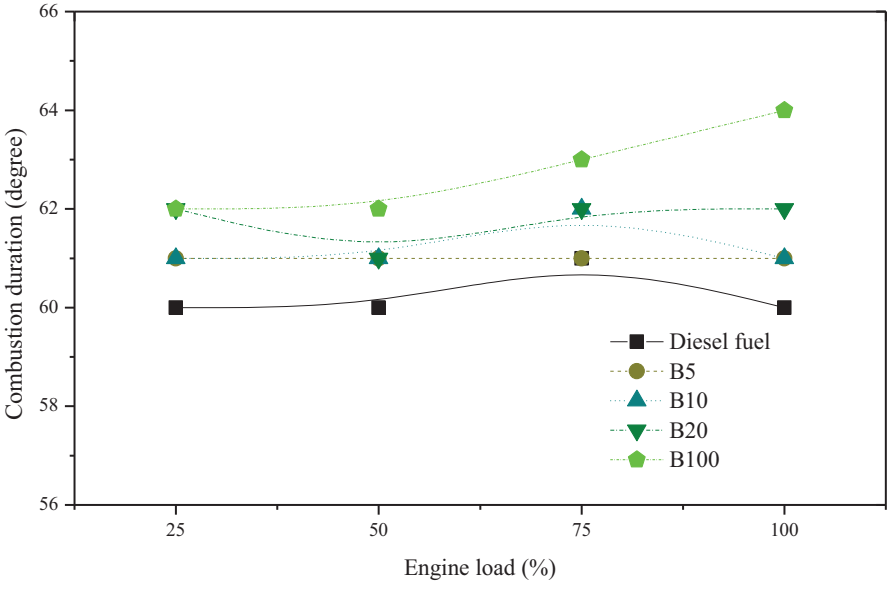

Fig. 9. The variation of CD with respect to the engine load for tested fuels.

baseline diesel fuel. In this study, the cetane values of the tested fuel samples were tabulated in Table 2. Considering the cetane numbers of the used fuels, it could be recorded that the IDP was longer for B100 and its blends when compared with traditional diesel fuel. This can be because of the lower cetane ratings of biodiesel and its blends. The second reason might be the presence of the oxygen molecule in the molecular structure of the biodiesel [98]. Furthermore, it was observed that there were degradations in the IDP for all test fuel samples with ascending the engine load. In conclusion, at 100% load operating condition, the IDP values for conventional diesel fuel, B100, B5, B10, and B20 were calculated to be 7 deg, 10 deg, 8 deg, 8 deg, and 9 deg, respectively.

5.1.6 Combustion duration

The change in the duration of the combustion process (CD) for different tested fuel samples according to the engine load was plotted in Figure 9. The experimental findings indicated that the CD values for biodiesel fuel blends were monitored to be slightly higher in comparison with the diesel fuel at all engine loads. The dispersion of the droplet dimension of the injected fuel sprayed ascended because

of the higher kinematic viscosity and lower volatility specifications of the biodiesel. In this perspective, the less volatile fuels including grand size droplets continue a longer duration to atomize the fuel and to mix with air. In this way, the further combustion process and also remarks are noteworthy throughout the late burning stage [84]. To conclude, the CD values would be comparatively increased when the infusion of even a small percentage of biodiesel fuel into the diesel. At 100% engine loading condition, the CD values were calculated to be 60 deg for conventional diesel fuel, 64 deg for B100, 61 deg for B5, 61 deg for B10, and 62 deg for B20. Pretty much identical outcomes were monitored by Shrivastava *et al.* [84] who found that both the usage of neat biodiesel and the addition of biodiesel into the diesel fuel would lead to an increase of the CD.

5.1.7 Mass fraction burned

The Mass Fraction Burned (MFB) is a normalized parameter with a scale from zero to one or 0–100% for each cycle of the engine, defining the process of emitted chemical energy depending upon the crank angle [99]. The behavior of the MFB for any fuel in an engine is also a basic index of the combustion process [13]. The cetane number, engine load, oxygen content, and the enthalpy of the vaporization are the reasons for the higher influence on the MFB framework [100]. In other words, the MFB is the quantity of fuel burnt in the combustion chamber. For the calculation of the MFB, the partial pressure rise method has been implemented in this analysis. The comparison of MFB concerning the crank angle for all tested fuel samples at the engine load of 100% was shown in Figure 10. The MFB plays a considerable role in understanding the pollutants released from the exhaust, efficiency, and total performance of the tested engine. It can be monitored that the MFB jumped in slightly up with ascending of the biodiesel concentration. This is ascribed to the high proportion of oxygen atoms in the blend of biodiesel, resulting in a high rate of combustion. By the way, the locations of 5% and 90% of the MFB graphs have been utilized to determine the SOC and EOC positions, respectively. Because of this, the intervals between the crank angle situations of 5% MFB and 90% MFB were used to define the CD, as above-mentioned. When Figure 10 was examined, it can be seen that diesel fuel showed a lower MFB in comparison with other tested fuel samples, however, the region regarding the flame out converged with other fuel blends 7 deg late crank angle. As a result, rich air/fuel mixture conditions are happened in the combustion chamber due to the lower oxygen content of diesel fuel. For that reason, a delayed or longer duration is necessary to occur enough pressure on account of burning the fuel massive thoroughly. Due to the inherent oxygen content in the ester bonds, B100 results in the earlier SOC generating higher MFB at positions of lower crank angles. In addition, at lower engine loads, some irregularities were monitored for biodiesel blends. The creation of charge-rich regions in the combustion chamber, low cetane ratings, and poor fuel atomization characteristics can be attached to the above-stated inconsistencies. Similar results were also found by Ramesh *et al.* [101] using

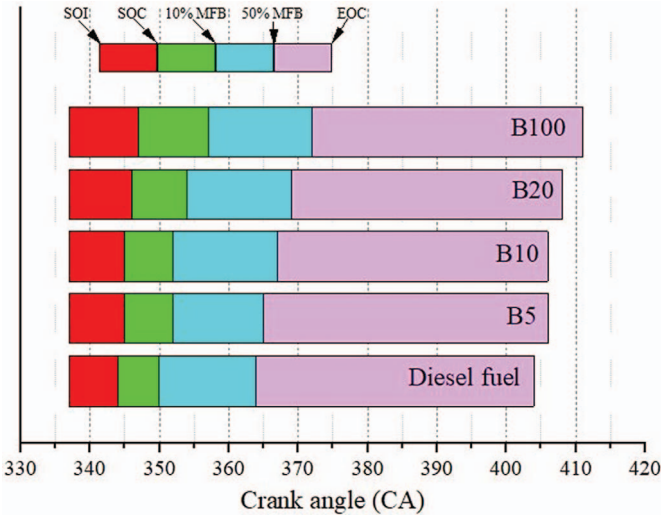

Fig. 10. The variation of MFB with respect to the engine load for tested fuels.

Calophyllum inophyllum biodiesel in a compression-ignition engine at various loads.

5.1.8 Mean gas temperature

Figure 11 shows the variation of the Mean Gas Temperature (MGT) of the tested fuels according to the crank angle at various engine loads. When the curves of the MGT were comprehensively evaluated, almost similar tendencies were observed with the EGT graph. The increase in the engine load caused to increase in the MGT for all tested fuels. Accordingly, the peak MGT values for the conventional diesel fuel, B5, B10, B20, and B100 were found to be 1244 °C, 1261 °C, 1351 °C, and 1479 °C respectively. As hoped, the maximum MGT figures of the biodiesel blends have been observed to be higher than unmodified diesel fuel due to the enhancement of the combustion process with the increase in the oxygen concentration in the combustion chamber coming from the biodiesel. The other reason for the high outcome of the biodiesel blends is that the CD values of the tested fuel samples are very close to each other [76].

5.1.9 Ringing intensity

A ringing operation with an extreme level leads to a higher combustion noise in the internal combustion engines. This case can result in detriments on various parts of the engine. Therefore, it is understandably remarkable to address the characteristics of the Ringing Intensity (RIN) since it expresses the combustion noise in the engine. Figure 12 illustrates the change in the RIN values at various engine loading conditions for tested fuel samples. It was suggested by Maurya and Saxena [102] that the RIN results should be lower than a specific value (5 MW/m^2), resulting in a convenient combustion noise level as well as free of operation from the knock event. Accordingly, the aforesaid grade has been used to be THE highest limit for receivable noise in the combustion process. In addition, the RIN is

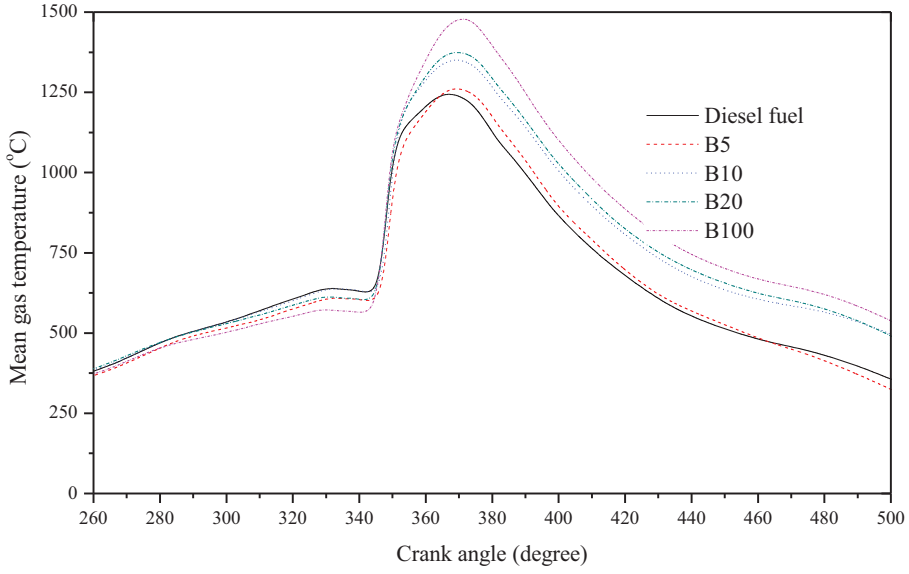

Fig. 11. The variation of MGT with respect to the engine load for tested fuels.

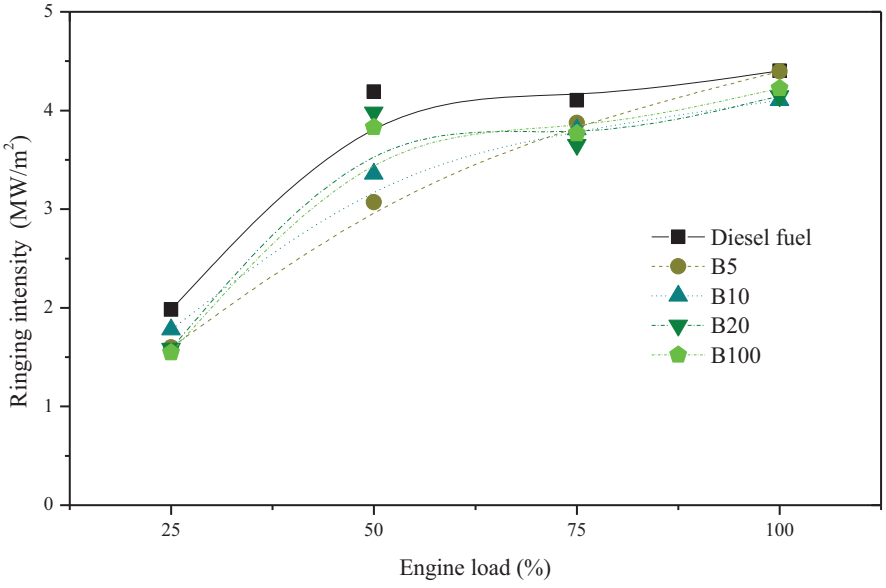

Fig. 12. The change in the RIN values at various engine loading conditions for tested fuel samples.

dependent upon the engine load, engine speed, maximum in-cylinder gas pressure, and peak PRR patterns [103]. As can be seen in Figure 12, the augmentation in the engine loads led to an increase of the RIN figures. The current work showed that the maximum RIN findings for conventional diesel fuel, B5, B10, B20, and B100 were computed to be 4.40 MW/m^2, 4.39 MW/m^2, 4.10 MW/m^2, 4.14 MW/m^2, and 4.23 MW/m^2, respectively. As observed, the highest RIN values at full load operation were monitored when the tested engine operated with traditional diesel fuel because of its high apparent HRR characteristics, as pointed out by Soloiu *et al.* [78]. As anticipated, the induction of alternating biodiesel fuel to the traditional diesel fuel provided reductions in the RIN values owing to the biodiesel's lubrication feature. Uludamar *et al.* [104], in their experimental research, for instance, remarked that the noise and vibration figures of the diesel engine deteriorated with the ascending percentages of biodiesel fuel in the tested mixtures. Overall, according to the present RIN outcomes, this present work demonstrated that the biodiesel produced from hemp seed crude oil caused to a reduction in vibration and noise as compared to diesel fuel operation. In addition, the authors have observed this event when the engine was operated with biodiesel. Erdoğan *et al.* [71] and Yesilyurt [105] reported that the RIN figures were achieved lower when the engine was fueled with biodiesel in comparison

with the diesel fuel because of the above-indicated reason. Soloiu *et al.* [106] stated that a lower RIN happened when the engine run on the neat biodiesel synthesized from cottonseed oil since the PRR for biodiesel fuel was lower by 20% than that of No. 2 diesel fuel. Uyumaz [8] pointed out that the RIN values descended with the rise of mustard oil biodiesel concentration in the fuel blends and the lowest RIN value was predicted with using diesel fuel. It could be accounted for the reason as the lower energy content of biodiesel led to a more consistent combustion process taking place in the engine cylinder.

To sum up, the considerable findings achieved from the present experiments regarding the combustion and ignition characteristics of the researched compression-ignition engine operating with the hemp seed oil methyl ester and its blends with diesel fuel appeared in Table 4 in detail. The following table also gives out the relative air-fuel ratio (λ) for all test fuels at various engine loading conditions with a constant engine speed of 1500 rpm. As observed, λ declined with loading because of the stable build-up operation. Initially, the stoichiometric air-fuel ratios for hemp seed oil methyl ester and conventional diesel fuel were computed to be 14.40 and..., respectively. In this regard, the combustion equation for the above-stated tested neat fuels were exhibited below.

- The combustion equation of hemp seed oil methyl ester:

$$C_{17.60}H_{30.47}O_2 + 25.2175(O_2 + 3.76N_2) \rightarrow 17.60CO_2 + 15.235H_2O + 94.8178N_2 \quad (15)$$

- The combustion equation of conventional diesel fuel:

$$C_{14}H_{25} + 20.25(O_2 + 3.76N_2) \rightarrow 14CO_2 + 12.5H_2O + 76.14N_2 \quad (16)$$

It is to be noted that the chemical formula of the conventional diesel fuel was adopted from Özgür [107] while the chemical formula of the hemp seed oil biodiesel was estimated from its fatty acid composition profile. In this context, the maximum relative air-fuel ratio was obtained to be 3.96 for base fuel under the lowest engine loading condition. The hemp seed oil biodiesel, as well as the test fuel mixtures, possessed lower λ values, corresponding to boosted consumption of fuel.

5.2 Harmful pollutant characteristics

In the following division of the present paper, the distinct harmful pollutant parameters like Carbon Monoxide (CO), Oxides of Nitrogen (NO_X), Carbon Dioxide (CO_2), Unburned Hydrocarbon (UHC), Oxygen (O_2), and smoke opacity emissions of a compression-ignition engine fueled with B100, B5, B10, and B20 have been investigated in detail and discussed in the point of the latest published papers in the literature. Furthermore, the results of the tested alternating fuels were compared with the traditional diesel fuel for better evaluations.

5.2.1 Carbon monoxide emission

Carbon Monoxide (CO) emission, which is one of the most considerable exhaust gases in the internal combustion engines, is an indicator of the deficient combustion process inside the cylinder on account of an insufficient figure of air in the fuel/air mixture or inadequate duration in the cycle for the achievement of the combustion reaction in the engine. Namely, it means briefly that the concentration of the CO emission is largely dependent on the working conditions of the engine and fuel/air ratio as well [108, 109]. Briefly, the combustion process with unsatisfactory procurement of oxygen happens in the formation of CO from the exhaust. The alteration of the CO emission values for B100 and its blends with conventional diesel fuel concerning the engine load is depicted in Figure 13. Based on the graph given in Figure 13, biodiesel-added diesel fuel blends emitted a lower amount of CO emission than that of baseline diesel fuel. Accordingly, the CO emission values for diesel fuel, B100, B5, B10, and B20 were measured to be on average 9.49 g/kW h, 4.91 g/kW h, 8.41 g/kW h, 7.31 g/kW h, and 6.17 g/kW h, respectively. As predicted, the augmentation of the biodiesel concentration in the fuel resulted in a lower amount of CO emission because of the presence of the oxygen molecule in the molecular structure of the biodiesel. The available findings match with those previously conducted research by various researchers. Damanik *et al.* [110], for instance, reviewed the relevance of the biodiesel blends for compression-ignition engines given their lower CO emission characteristics in the exhaust of the diesel engine. Qi *et al.* [88] pointed out that the CO emissions of biodiesel and its blends with diesel fuel were measured to be low owing to the existence of additional oxygen molecules in the chemical structure of the tested biodiesel. It was approximately 40% lower than diesel fuel. Chauhan *et al.* [87] reported that a smaller amount of CO emissions was emitted from the exhaust when the diesel engine was fueled with Jatropha oil methyl ester and its blends with diesel fuel during the experimentations as compared to neat diesel fuel. Similarly, Silitonga *et al.* [111] highlighted that the CO emissions were measured to be lower when the engine operated with bioethanol–biodiesel–diesel fuel alternating blends under a full-throttle opening condition.

5.2.2 Oxides of nitrogen emission

Figure 14 portrayed the alteration in the Oxides of Nitrogen (NO_X) by all tested fuel samples at different engine loading conditions. When the graph was examined, it was to be noticed that the pure biodiesel and its blends formed a higher amount of NO_X emission by approximately 16.54–65.87% in contrast to the conventional diesel fuel at the load of 25% to full load. On average, entire biodiesel–diesel test fuels used in this experimental research produced higher NO_X emissions in comparison with the base fuel. Accordingly, the averaged NO_X emissions for diesel fuel, B5, B10, B20, and B100 were found to be at 6.83 g/kW h, 7.96 g/kW h, 8.85 g/kW h, 9.76 g/kW h, and 11.34 g/kW h, respectively. This can be explained as the influence of the excessive amount of oxygen molecules in

Table 4. The considerable injection and combustion parameters coming from the analyses in this study.

Engine load	Fuel types	SOI (deg)	FLP_{max} (bar)	IDP (deg)	SOC (deg)	EOC	ACP_{max} (deg)	CP_{max} (bar)	AIP_{max} (deg)	PRR_{max} (bar/deg)	MGT_{max} (°C)	$AMGT_{max}$ (deg)	λ (–)	$AHRR_{max}$ (deg)	HRR_{max} (J/deg)	$ACHR_{max}$ (deg)	CHR_{max} (kJ)
25%	D100	337	212.36	12	349	409	365	64.91	354	3.7	1124	373	1.86	354	46.3	477	1.15
	B5	338	206.52	12	350	411	366	62.99	354	3.3	1082	374	1.33	354	40.7	476	1.12
	B10	337	221.07	13	350	411	368	61.70	354	3.4	1154	375	1.26	354	41.1	421	0.75
	B20	337	218.71	13	350	412	368	59.95	354	3.2	1093	374	1.19	354	39.8	422	0.74
	B100	337	227.21	14	351	413	370	59.24	354	3.1	1165	375	1.13	354	39.6	418	0.73
50%	D100	336	217.82	10	346	406	363	73.06	351	5.7	1133	375	1.85	351	47.3	476	1.42
	B5	337	202.89	10	347	408	365	70.60	352	4.7	1252	375	1.79	352	47.1	475	1.38
	B10	336	209.72	11	347	408	368	71.59	352	4.9	1315	375	1.77	352	46.9	421	0.83
	B20	337	215.78	11	348	409	369	69.73	352	5.3	1273	375	1.59	352	44.2	422	0.82
	B100	336	235.31	12	348	410	369	68.64	352	5.1	1346	376	1.54	352	41.5	412	0.82
75%	D100	336	219.11	8	344	405	366	79.74	351	5.7	1333	376	2.57	351	50.3	477	1.21
	B5	337	213.54	9	346	407	366	77.58	351	5.4	1410	375	2.46	351	50.1	476	1.13
	B10	336	207.37	10	346	408	367	75.78	351	5.3	1397	375	2.42	351	48.5	418	1.11
	B20	337	212.81	10	347	409	368	76.43	351	5.2	1415	375	2.04	351	47.3	427	1.01
	B100	336	223.16	11	347	410	390	75.18	351	5.2	1463	375	2.02	351	46.5	419	0.91
100%	D100	337	223.39	7	344	404	366	85.44	365	6.2	1244	367	3.46	350	77.82	475	1.12
	B5	337	230.91	8	345	406	367	83.28	365	6.1	1261	369	3.41	350	76.79	474	1.00
	B10	337	234.69	8	345	406	367	83.04	365	5.8	1351	369	3.35	350	75.46	419	0.82
	B20	337	230.01	9	346	408	368	82.72	366	5.8	1374	369	2.78	350	69.53	423	0.78
	B100	337	234.23	10	347	411	368	80.85	366	5.7	1479	371	2.68	351	66.73	415	0.76

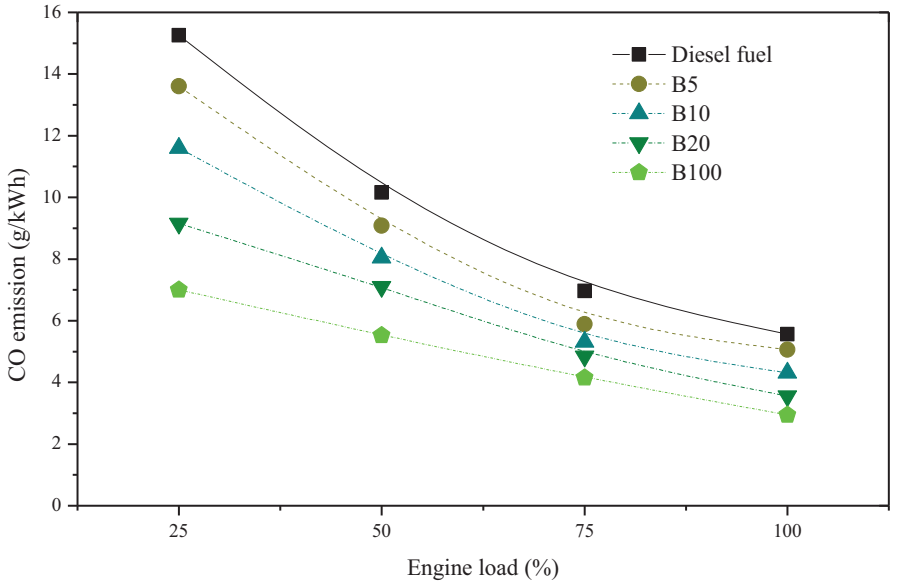

Fig. 13. The change in the CO emissions at various engine loading conditions for tested fuel samples.

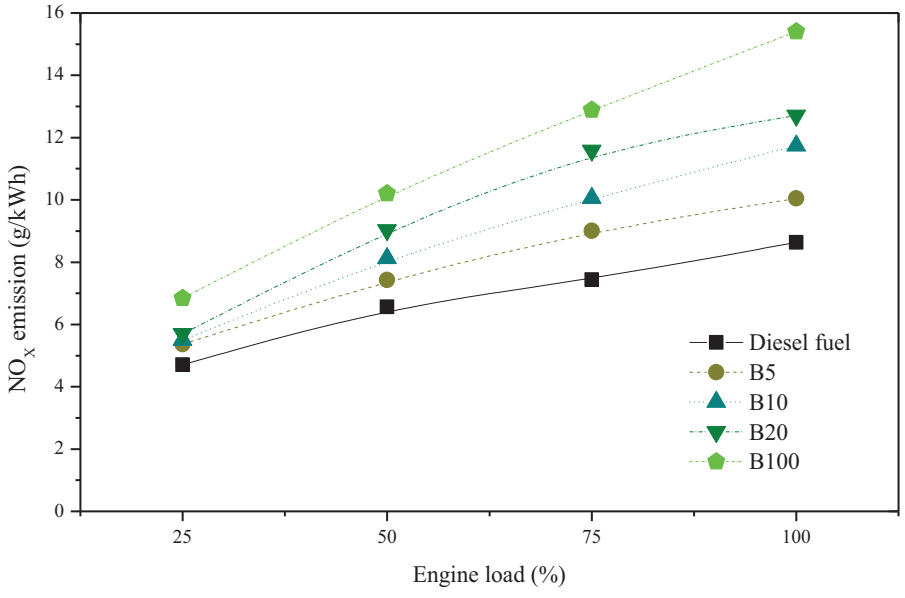

Fig. 14. Variation of NO_X emission values in relation to engine load for tested fuels.

the combustion chamber of the engine coming from the biodiesel utilization that improved the combustion efficiency resulting in the increase of the combustion temperature in the cylinder. Besides that, the NO_X emissions increased because of the augmented temperature inside the cylinder at higher engine loads in comparison with the lower loads. The above-mentioned reason can be verified when in-cylinder gas temperature and exhaust gas temperature were examined. It is to be noted that more fuel was consumed during the combustion reaction inside the cylinder because more oxygen molecule is ensured to the cylinder on account of the infusion of biodiesel as an oxygenated additive. As is well-known, one of the most significant parameters that affect nitrogen oxides formation is temperature. The other parameter on the generation of nitrogen oxides is the longer duration of the combustion process inside the cylinder [112]. The oxides of nitrogen emissions formation by combining oxygen and nitrogen depend upon the oxygen concentration, residual time, and combustion temperature which have been explained in the Zeldovich mechanism [113]. As will be mentioned in the following sections, BSFC figures for biodiesel and its blends were higher than that of base fuel which indicated the occurrence of a higher cylinder temperature for biodiesel and its mixtures in comparison with the diesel fuel. The EGT curves can be an indicator of this knowledge. Additionally, the quantity of the produced nitrogen oxides

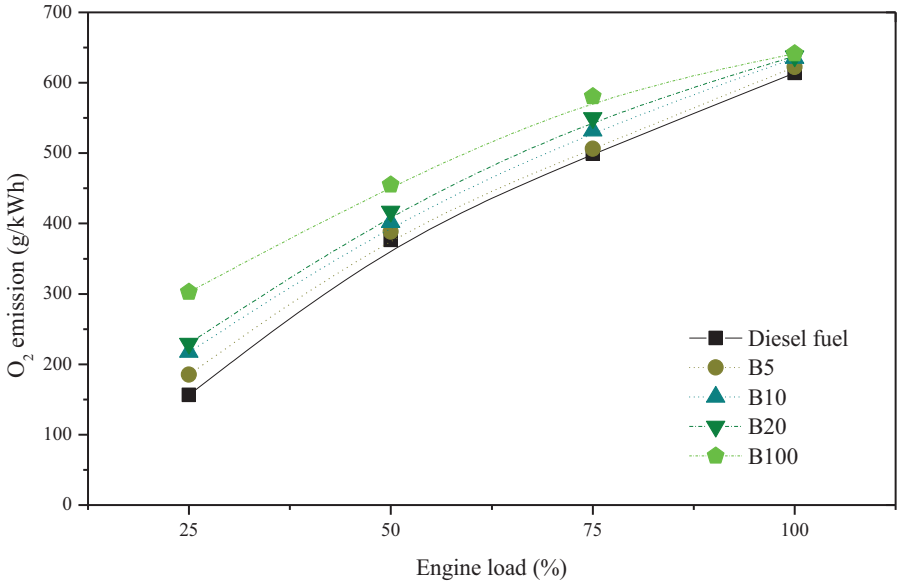

Fig. 15. Variation of O_2 emission values in relation to engine load for tested fuels.

emissions was also susceptible to the place within the combustion chamber. Accordingly, the maximum generation generally occurs close to the fuel injector since the pressure and temperature have been highest in there. In other words, nitrogen oxides emissions increase because of the reaction between oxygen and nitrogen at elevated temperature conditions depending on the ascending temperature in the chamber of the combustion [114]. The outcomes coming from the present measurements are in line with the monitoring of various authors. Asokan *et al.* [62], for instance, found that juliflora oil biodiesel produced slightly higher NO_X emissions as compared to diesel fuel at the highest engine loading condition. Özener *et al.* [115] followed that the generation of NO_X for biodiesel fuel was found to be 17.62% higher than diesel fuel under full loading. Chauhan *et al.* [87] indicated that the NO_X emissions emitted from the diesel engine running on the Jatropha oil biodiesel and its blends as higher than those of diesel fuel. Nabi *et al.* [116] pointed out that the formation of NO_X emissions was augmented using biodiesel in contrast to the conventional diesel fuel because of the higher concentration of oxygen content located in the chemical structure of the biodiesel. Canakci [117] showed that the utilization of biodiesel and its blends in the diesel engine led to an increase of the NO_X emissions by approximately 11.2%.

5.2.3 Oxygen emission

Figure 15 presented the variation of the O_2 emissions for biodiesel and its blends with diesel fuel across several engine loads with a constant speed of 1500 rpm. As observed from the graph, the O_2 emission values were obtained quite low because of the more complete combustion reaction taking place inside the cylinder. The average O_2 emissions for B100, B5, B10, B20, and mineral diesel fuel were found to be at 495.01 g/kW h, 425.62 g/kW h, 446.44 g/kW h, 458.75 g/kW h, and 411.47 g/kW h respectively. The use of biodiesel and the addition of a higher amount of biodiesel into diesel led to generating a higher concentration of O_2 emission because of the inherent oxygen molecules of biodiesel [118].

5.2.4 Unburned hydrocarbon emission

The Unburned Hydrocarbon (UHC) emission or more appropriately organic emissions have been pointed out as a by-product considering the uncompleted combustion reaction of the hydrocarbon fuel in the cylinder [119]. As a matter of fact that the UHC emission has referred to the lost chemical energy at which cannot completely convert to the available work in the internal combustion engines [120]. Furthermore, the UHC emission level in the exhaust gases was specified given the total hydrocarbon in general [119]. What is more, UHC emission is the major contributor to photochemical smog and ozone pollution as well [112]. The change in the unburned HC emissions released from the tested compression-ignition engine when it was run on biodiesel and its blends with diesel fuel at a load ranging from low to high for 1500 rpm were depicted in Figure 16. The basic reason for the generation of UHC is a lower cylinder temperature and deficient combustion process [62]. As can be seen in the graph given underneath, it showed a fluctuating trend reaching the maximum load and the highest measurements were realized at the load of 100% for all tested fuels. Moreover, the usage of biodiesel and its blends resulted in a decrement in the UHC emission levels as compared to base fuel. At the highest engine load, the maximum UHC emission values for base fuel, B5, B10, B20, and B100 were found to be at 0.82 g/kW h, 0.65 g/kW h, 0.35 g/kW h, 0.20 g/kW h, and 0.10 g/kW h, respectively. If all the obtained results from 25% to full load were evaluated according to the diesel fuel, 5%, 10%, and 20% biodiesel addition into diesel caused reductions approximately by 29.54%, 47.07%, and 63.15%,

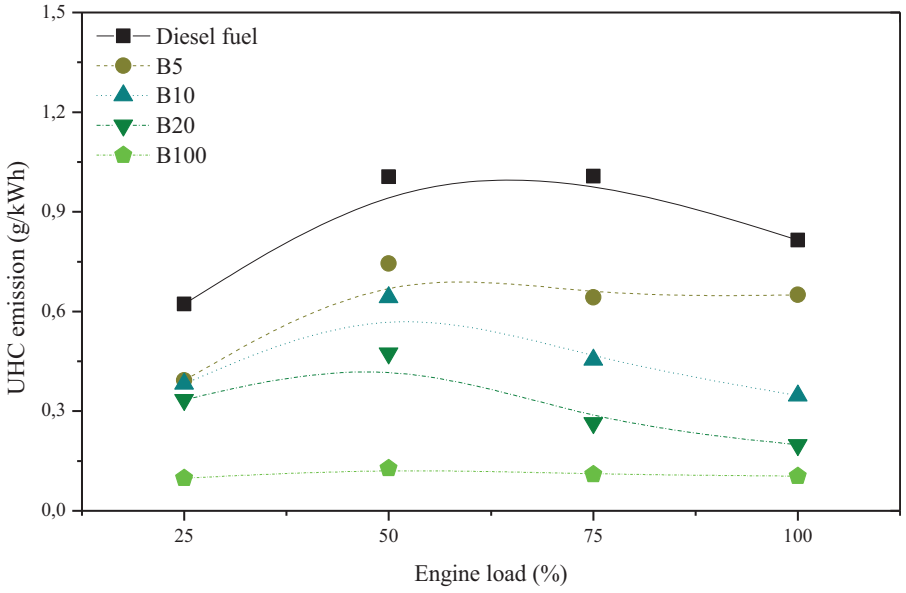

Fig. 16. Variation of UHC emission values in relation to engine load for tested fuels.

respectively. In addition, it was observed that the smallest value was measured for B100 amongst other tested fuels. This case may be explained that when biodiesel blends were used in the engine, more oxygen atoms enter the combustion reaction because biodiesel has an excessive amount of oxygen in its chemical bond, as stated in Table 2. Accordingly, the higher oxygen concentration in the combustion chamber causes more complete burning of the fuel [62]. The results and their arguments were also consistent with the outcomes presented by previous researchers. Some of them were briefly explained as follows: Chauhan *et al.* [87], for instance, indicated that the UHC emissions from the compression-ignition engine operating with Jatropha oil biodiesel and its blends were observed to be less than diesel fuel operation. Enweremadu and Rutto [121] reviewed that the usage of used cooking oil biodiesel resulted in a lower concentration of UHC from the engine. Pinzi *et al.* [122] pointed out a decrement in UHC emission as the consequence of the augmented proportion of short-chain and saturated fatty acid methyl esters in the composition of biodiesel. Damanik *et al.* [110] approved in their considerable review paper that most of the biodiesel blends have exhibited substantial reductions in the UHC emissions of the compression-ignition engine.

5.2.5 Carbon dioxide emission

The Carbon Dioxide (CO_2) emission is accepted as one of the undesired emissions in terms of its remarkable contribution to global warming. On the other hand, CO_2 emission is a very important gas for internal combustion engines because it implies the complete combustion process. The effect of the variation of biodiesel concentration in the blend and engine load for test engine on the CO_2 emission changing were illustrated in Figure 17. From the graph, it is to be noted that the generation of CO_2 emission for used fuels in this study is less sensitive to the increase in the engine load along with the biodiesel fraction in the blend. In other words, base diesel fuel and biodiesel–diesel fuel blends generated almost similar CO_2 emission levels in all engine loading conditions, and hence, there is no statistically apparent influence by the infusion of biodiesel fuel into the diesel on the CO_2 emission up to 20% ratios by volume. On average, the CO_2 emission figures for traditional diesel fuel, B5, B10, B20, and B100 were achieved to be 240.96 g/kW h, 250.08 g/kW h, 263.10 g/kW h, 278.66 g/kW h, and 389.14 g/kW h, respectively. As estimated, the CO_2 emissions trends were found to be similar for each fuel sample. Restated briefly, the treatment of base fuel with the application of hemp seed oil biodiesel caused to increase in the oxygen molecules in the mixtures due to the excess amount of oxygen content in the biodiesel resulting in less UHC and CO emissions but increased the CO_2 emission. From a different point of view, the CO_2 gas is not taken into account as a harmful pollutant since it can natively be recycled and generate oxygen, however, if the concentration of the CO_2 level overlaps the recommended limit, which is 5000 ppm, then it poses a potential health hazard [123]. Ascending in the CO_2 emission is owing to the influence of oxygen concentration rises that contributes to increasing the ratio of the complete combustion reaction. As a result, the increase of oxygen atoms in the combustion chamber will lead to more carbon which can be transformed into CO_2 gases [119]. Numerous researches were carried out by using biodiesel synthesized various types of raw materials in the recent literature. Some of them were summarized to validate the present findings as follows: Uyumaz [63], for example, reported that CO_2 and CO emissions were enormously affected by the infusion of biodiesel, and the higher oxygen content of biodiesel in its chemical structure caused to decline the CO and increase CO_2 emissions because the oxidation process enhanced depending upon the oxygen

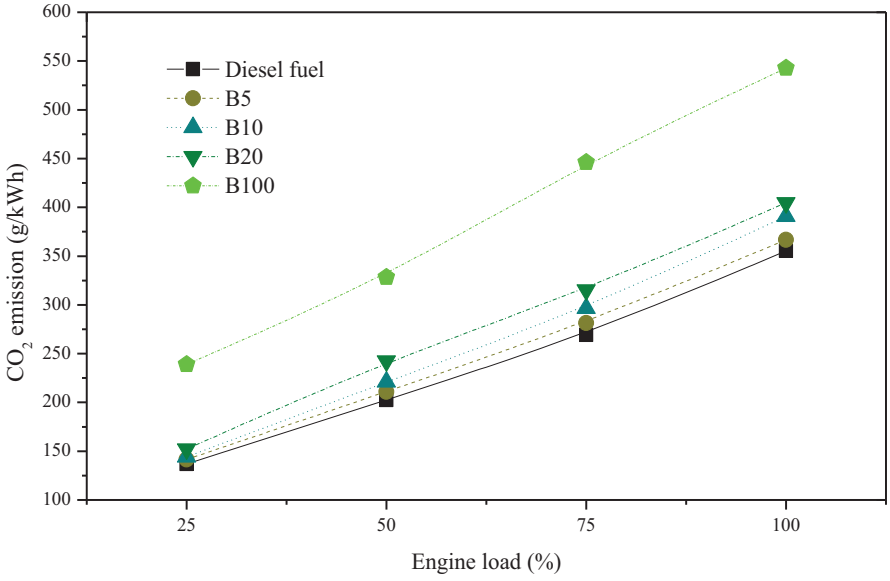

Fig. 17. Variation of CO_2 emission values in relation to engine load for tested fuels.

molecules. Yesilyurt [105] highlighted that neat peanut oil methyl ester emitted the highest CO_2 emissions among the tested fuels at all operating conditions while the mineral diesel released the lowest one because of its higher energy content, improved the efficiency characteristics and even atomization behaviors of the fuel's droplet size led to a decrease of the CO_2 emission levels. Özener *et al.* [115] observed that fueling the tested engine with pure soybean oil biodiesel ascended the CO_2 formation by approximately 5.63% and fueling with the B50 ascended the CO_2 formation by approximately 2.77% while the usage of B10 and B20 blends did not have a considerable influence on the CO_2 emission levels according to the diesel fuel operation.

5.2.6 Smoke opacity

Smoke is the outcome of the incomplete combustion reaction and is generated at the region having a rich zone in the combustion chamber [124]. Figure 18 displays the alteration of smoke opacity values about the engine loads for tested fuels of biodiesel, diesel fuel, and their various binary blends. As known, the amount of the smoke emitted from the compression-ignition engines' exhaust can be computed as a smoke opacity. The oxygen content of the fuel is the key parameter that influences the smoke opacity. A large amount of smoke is spread out through the agency of the exhaust as a consequence of the oxygen throughout the combustion process. In the present study, the mean smoke opacity values at the ranged operating condition for conventional diesel fuel, B5, B10, B20, and neat hemp seed oil biodiesel were measured to be 1.23 1/m, 0.98 1/m, 0.62 1/m, 0.48 1/m, and 0.43 1/m, respectively. Contrary to the reference fuel, the smoke opacity figures were observed to be lower for biodiesel blends at all engine operating statuses. This is due to the presence of the oxygen molecule in the molecular structure of the hemp seed oil biodiesel, which helps the fracture of the aromatic contents [62]. Silitonga *et al.* [111] indicated that the utilization of biodiesel–bioethanol–diesel alternating blends in the diesel engine caused to decrease in the smoke opacity values when the tested engine operated at full throttle condition. However, the usage of pure biodiesel in the engine resulted in augmented aromatics, which gave higher smoke.

5.3 Performance characteristics

The variation of the engine performance characteristics by different loading conditions has been performed by the evaluation of the following parameters: Brake Specific Fuel Consumption (BSFC), Brake Specific Energy Consumption (BSEC), and Exhaust Gas Temperature (EGT). By the way, an important point needs to be mentioned that the engine speed was selected to be 1500 rpm which is the provided speed from the manufacturer. The engine torque can be described as the ability to do work for the engines. Since the charging rate into the cylinder is less as well as the conditions of the combustion process happen suboptimal at low and high engine speed, the torque value occurs low in the internal combustion engines. Therefore, the most beneficial operating conditions can be acquired at medium engine speeds. From this perspective, the present study was conducted at a particular engine speed of 1500 rpm. The findings of the above-mentioned parameters have been discussed in detail in the subsections as given underneath for all the test fuel specimens (diesel, B5, B10, B20, and B100) taking into consideration the latest literature knowledge. Additionally, it could be monitored that the utilization of pure hemp seed oil biodiesel did not cause that the tested engine was commenced difficulty. On the other hand, the engine operated irregularly at higher engine speeds.

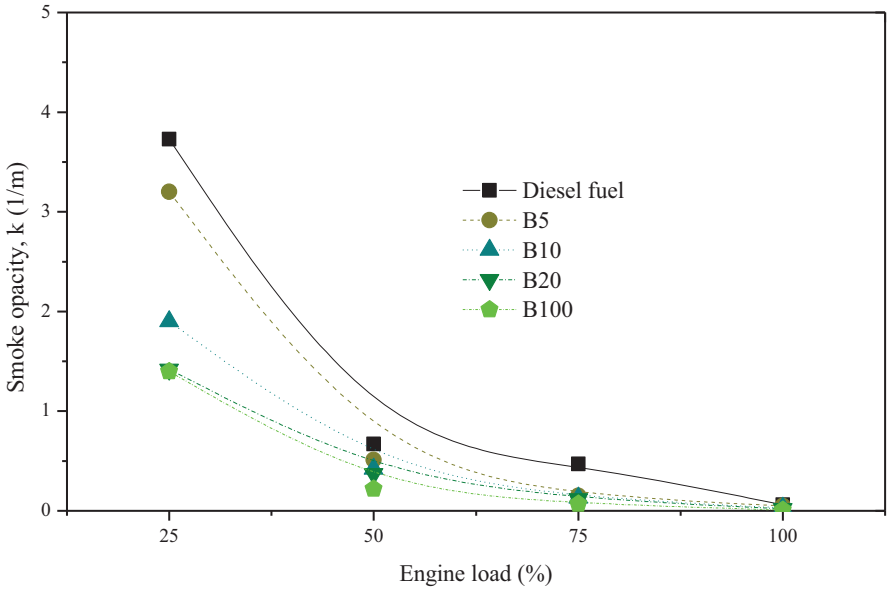

Fig. 18. Variation of smoke opacity values in relation to engine load for tested fuels.

5.3.1 Brake specific fuel consumption

The Brake Specific Fuel Consumption (BSFC) is characterized as the quantity of necessary fuel to effectuate 1 kW of brake power in 1 h; namely, it clarifies the efficiency of the used fuel for any internal combustion engine. For this reason, BSFC plays a vital role in the selection of parameters for any recommended fuel specimen. The BSFC figures of the tested fuels for the current study were calculated using equation (5). Figure 19 illustrates the alteration of the BSFC results for pure biodiesel fuel and its different blends with the baseline diesel fuel according to the various engine load conditions. The BSFC outcomes for all test fuels dropped when the engine was loaded from 25% to 100% in the steps of 25%. Accordingly, the lowest BSFC values were obtained to be the highest engine load. Besides that, in the conducted trials, it was detected that the highest BSFC figures were monitored with B100 alternating fuel meanwhile the least BSFC results were observed with diesel fuel. This is because of the lower energy content of the biodiesel. As seen in Table 2, the lower calorific value of the reference diesel fuel (43.850 MJ/kg) is much higher than that of biodiesel (38.737 MJ/kg). In light of this knowledge, the biodiesel concentration in the fuel blend influenced the fuel consumption of the tested compression-ignition engine. Because the lower calorific value of diesel is approximately 1.13 times higher than biodiesel, it was determined that the BSFC ascended to ensure the identical network outlet in the engine as the biodiesel proportion in the mixture augmented from 5% to 100%. It is to be noted that the minimum BSFC values for diesel, B5, B10, B20, and B100 were found to be at 0.275 kg/kW h, 0.291 kg/kW h, 0.305 kg/kW h, 0.312 kg/kW h, and 0.372 kg/kW h, respectively. As assumed, the energy content of the fuels ensured a major contribution to discuss the consumption of fuel. As is well-known, biodiesel fuels have a higher percentage of oxygen content in their chemical structure, as described in Table 2. Asokan *et al.* [62] reported that the usage of clear juliflora oil biodiesel was greater than that of diesel fuel owing to the lower energy content of biodiesel. Another reason for occurring higher BSFC in the use of biodiesel has been presented by Mofijur *et al.* [125]. The researchers marked that the BSFC figures for neat biodiesel and its blends were calculated to be higher than diesel fuel because of the integrated influences of viscosity, density, and the energy content of the tested fuels. Interestingly, Canakci [117] observed the BSFC for pure soybean oil biodiesel as slightly higher than reference diesel fuel. Özener *et al.* [115] reported that the increase of soybean oil biodiesel concentration in the test fuel from 10% to 100% resulted in ascending on BSFC by 2–9% in comparison with the diesel fuel. Chauhan *et al.* [87] exhibited the higher values in the BSFC for Jatropha oil biodiesel and its blends as compared to diesel fuel because of the higher density feature of the biodiesel.

5.3.2 Brake specific energy consumption

The Brake Specific Energy Consumption (BSEC) can be identified as the ratio of the energy ensured by employing fuel during 1 h to the composing unit net power [126]. The main characteristic that distinguishes BSEC from BSFC is the most certain factor to make comparison the capacity of any internal combustion engine operating with the various alternating fuel specimens including several thermal values and densities as well. As stated, BSEC can directly correlate with the BSFC figures for the test fuels. To sum up, the BSEC can be found considering the energy content and BSFC results for each fuel [127, 128]. To give an instance, the BSEC can be calculated using equation (6). The change in the BSEC figures for all tested fuel samples (pure biodiesel, B5, B10, B20, and conventional diesel fuel) regarding the engine load was portrayed in Figure 20. As hoped, the trend of the BSEC values

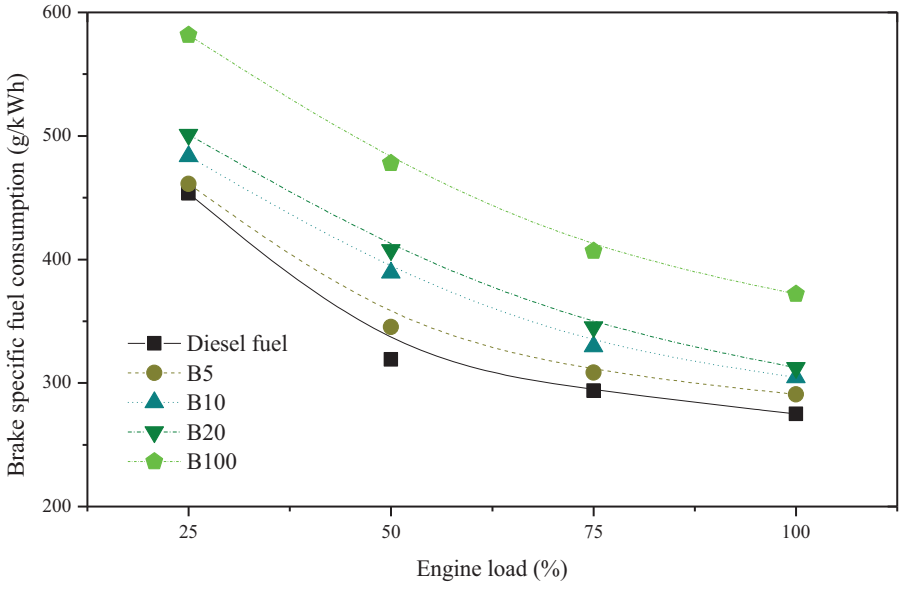

Fig. 19. Comparison of BSFC versus engine load for different fuels.

declined with the augmentation of engine load since the identical gradients were also monitored for the BSFC graphs as seen in Figure 19. In addition, the BSEC outcomes aligned with the opposite contour of the brake thermal efficiency, which was elaborately explained in the following section. As assumed, it is to be noticed that the BSEC findings for diesel fuel were the least by the other tested fuels across entire engine loading conditions. On the other hand, it is evident from the figure that the biodiesel and its blends had higher BSEC values because of the higher BSFC results, as observed in Figure 19. The lowest BSEC figures were found to be at the engine load of 100% as 12.06 MJ/kW h for conventional diesel fuel, 12.68 MJ/kW h for B5, 13.20 MJ/kW h for B10, 13.69 MJ/kW h for B20, and 14.42 MJ/kW h for B100. To the best of the authors' knowledge, there is a limited number of studies concerning the BSEC outcomes for alternative fuel blends in the literature. On the other hand, a few of them would be briefly explained as follows: Feng *et al.* [129], however, mentioned that positive findings regarding the BSEC, engine torque, HC emission, and CO emission were obtained from the tested engine with the application of 35% butanol and 1% H_2O when using the modified ignition timing. The researchers also stated that the BSEC was influenced by engine working conditions and fuel specifications; nonetheless, this outcome was restricted to the used engine, thus it is necessary to be further research to verify by more investigations.

5.3.3 Brake thermal efficiency

The Brake Thermal Efficiency (BTE) or sometimes called energetic efficiency defines the cases of the regular transformation operation of the heat energy to the useful mechanical network. The BTE of hemp seed oil biodiesel, conventional diesel fuel, and their binary blends at different engine working conditions are presented in Figure 21. As observed, the BTE curves for all tested fuels increased gradually with the increase in the load. A higher density, higher viscosity, and lower air/fuel mixture of the biodiesel fuel lead to a decrease of the BTE in the modes of using a higher percentage of biodiesel in the blend in comparison with the diesel fuel operation because of its aforesaid specifications which could be the reason to acquire a lower BTE at lower engine loads [62]. On the other hand, the BTE values for all tested fuel samples exhibited a similar tendency at higher engine loads. In this regard, the maximum BTE figures were obtained to be at the maximum engine load of 100%. In this load, the BTE for hemp seed oil biodiesel, diesel fuel, and their blends of B5, B10, and B20 were calculated to be 24.97%, 29.85%, 28.40%, 27.28%, and 26.91%, respectively. These findings and their related reasons were well matched with researches performed by Silitonga *et al.* [130] and Asokan *et al.* [62]. The BTE outcomes for lower concentration biodiesel blends were very close to diesel fuel and ascribed to the presence of inherent oxygen content of the biodiesel fuel, resulting in the improvement of the combustion efficiency in the engine. In addition, the elevated temperature of the air under higher engine loading conditions also leads to a mixing and better evaporation for biodiesel.

5.3.4 Exhaust gas temperature

The fuel properties such as density, energy content, cetane number, and kinematic viscosity have a potential influence on the Exhaust Gas Temperature (EGT) [131]. On the other, the EGT is a remarkable factor that affects harmful pollutants [132]. Figure 22 exhibits the EGT distribution with the operated engine loads for B100, traditional diesel fuel, and their different blends (B5, B10, and B20). It was monitored that the EGT ascends with the increase in the engine load gradually for all tested fuels. Previous studies have also presented an increase in the EGT figures with

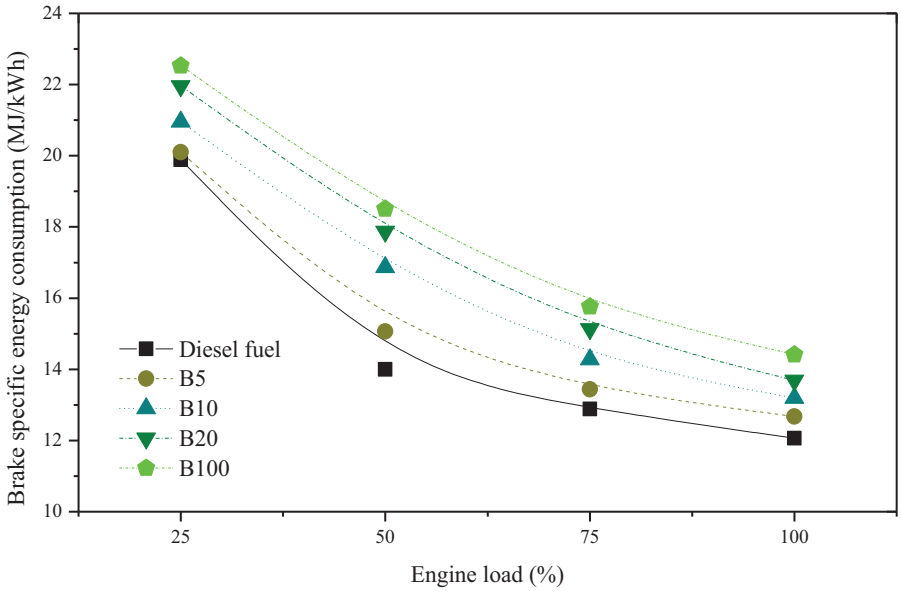

Fig. 20. Comparison of BSEC versus engine load for different fuels.

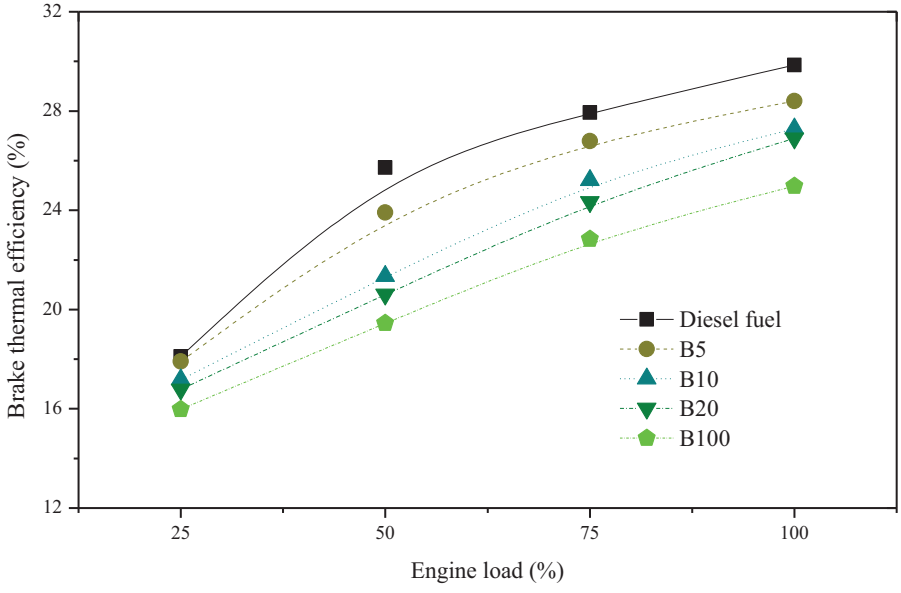

Fig. 21. Comparison of BTE versus engine load for different fuels.

an increase in engine speed as well as engine load [133–135]. This case can be explained that the amount of the test fuel injected into the combustion chamber boosts with regards to the load ascends and it leads to a higher temperature in the cylinder [136]. However, there was no considerable change in the EGT figure at each load for test fuel samples. Ramadhas *et al.* [67] also reported that the EGT was seen to be very close to that of baseline diesel fuel when the utilization of rubber seed oil as a fuel in the compression-ignition engine. The biodiesel content in the blend resulted in increasing the EGT because of more complete combustion process takes place inside the cylinder due to the excessive amount of oxygen concentration located in the chemical structure of the biodiesel. At the highest engine load, the EGT figures for mineral diesel fuel, B5, B10, B20, and B100 were found to be at 439.7 °C, 442.5 °C, 444.0 °C, 451.8 °C, and 454.6 °C, respectively. The heavier molecules of alternating biodiesel fuel cause a continuous combustion phase even throughout the exhaust stroke which results in a higher EGT [137, 138]. Panwar *et al.* [139] and Devan and Mahalakshmi [140] pointed out that the high viscosity properties of biodiesel/diesel fuel blends resulted in becoming poor combustion characteristics. For that reason, higher EGT could be happened owing to the increase in the duration of the burning stage. Onoji *et al.* [42] indicated that the EGT profile of various biodiesel/diesel fuel blends

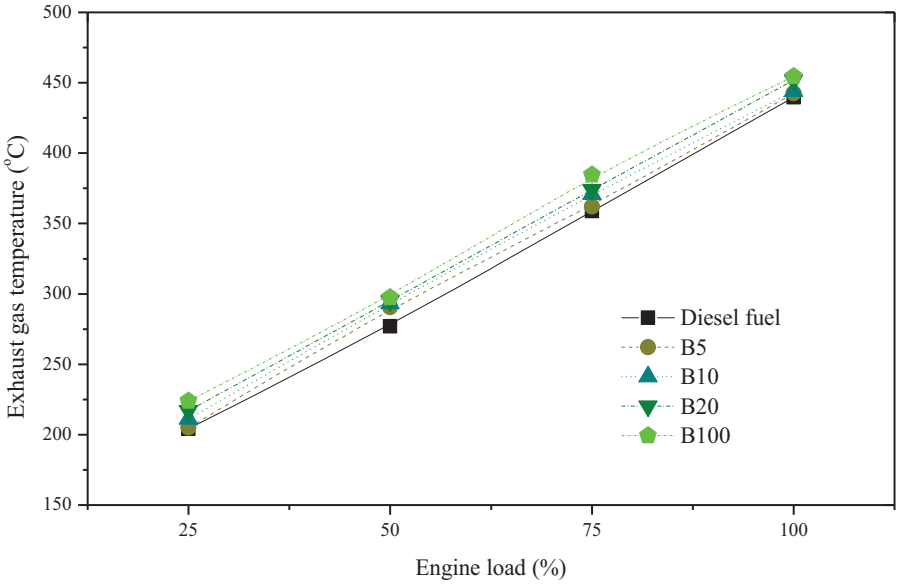

Fig. 22. Comparison of EGT versus engine load for different fuels.

Table 5. Comparative analyses of the experimental outcomes (from highest to lowest).

Characteristic	Parameter	Order
Combustion behavior	Peak in-cylinder pressure	Diesel fuel > B5 > B10 > B20 > B100
	Peak heat release rate	Diesel fuel > B5 > B10 > B20 > B100
	Ignition delay period	B100 > B20 > B10 > B5 > Diesel fuel
Harmful pollutants	Oxides of nitrogen	B100 > B20 > B10 > B5 > Diesel fuel
	Carbon dioxide	B100 > B20 > B10 > B5 > Diesel fuel
	Smoke opacity	Diesel fuel > B5 > B10 > B20 > B100
	Unburned hydrocarbon	Diesel fuel > B5 > B10 > B20 > B100
	Oxygen	B100 > B20 > B10 > B5 > Diesel fuel
	Carbon monoxide	Diesel fuel > B5 > B10 > B20 > B100
Engine performance	Brake thermal efficiency	Diesel fuel > B5 > B10 > B20 > B100
	Brake specific fuel consumption	B100 > B20 > B10 > B5 > Diesel fuel
	Brake specific energy consumption	B100 > B20 > B10 > B5 > Diesel fuel
	Exhaust gas temperature	B100 > B20 > B10 > B5 > Diesel fuel

demonstrated an upward trend with an increasing biodiesel percentage in the mixture because the ester molecule includes oxygen atoms which improve the combustion process. It is to be notified by Asokan *et al.* [58] that owing to the high viscosity specification of biodiesel, traces of unburnt fuel would be existent in the premixed burning stage that would proceed to burn and hence the EGT will increase progressively.

6 Overall evaluation of the present outcomes with recent investigations

Table 5 presents the comparative analyses of the findings (from highest to lowest) coming from the experimentations of the compression-ignition engine running on the hemp seed oil biodiesel and its blends with traditional diesel fuel at the engine load of 100% with a fixed speed of 1500 rpm. As can be seen in Table 5, the combustion behaviors, harmful pollutants, and engine performance parameters for all test fuels have been meticulously compared with each other. The entire parameters have been shown in the descended order for better assessment.

In addition, the outcomes acquired from the current research have been also compared with some similar and previously performed investigations and they have been tabulated in Table 6. The scrutinizations on the compression-ignition engines powered by the pure biodiesel fuels synthesized various alternating vegetable-based oils and their blends by different concentrations with diesel fuel have been represented on account of better evaluation of the present motivation. There is no doubt that several combinations

Table 6. Overall comparison of the present findings with other previously conducted researches.

Parameter	Present study	Uyumaz [63]	Uyumaz *et al.* [141]	Das *et al.* [142]	Sarıdemir and Ağbulut [3]	Tayari *et al.* [143]	Uyumaz [8]	Ashok *et al.* [127]	Asokan *et al.* [62]	Asokan *et al.* [58]	Dhar and Agarwal [86]	Raman *et al.* [144]
Base fuel	Diesel fuel	Diesel fuel	Diesel fuel	Diesel fuel	Diesel fuel	Diesel fuel	Diesel fuel	Diesel fuel	Diesel fuel	Diesel fuel	Diesel fuel	Diesel fuel
Raw material used in the biodiesel production	Hemp seed oil	Linseed oil	Poppy seed oil	Castor oil	Cottonseed oil	*Eruca sativa* seed oil	Mustard seed oil	*Calophyllum inophyllum* seed oil	Juliflora seed oil	Mixing of papaya and watermelon seed oils (50:50 ratio)	Karanja seed oil	Rapeseed oil
Types of test fuel	As a pure form and binary blends	As binary blends	As binary blends	As binary blends	As binary blends	As binary blends	As binary blends	As a pure form and binary blends	As a pure form and binary blends	As a pure form and binary blends	As a pure form and binary blends	As a pure form and binary blends
Proportions	5, 10, 20, and 100%	10, 20, and 30%	10 and 20%	5, 10, and 20%	10, 20, and 50%	2, 5, 10, 15, and 20%	10, 20, and 30%	30, 60, and 100%	20, 30, 40, and 100%	20, 30, 40, and 100%	5, 10, 20, 50, and 100%	25, 50, 75, and 100%
Type of test engine	Single-cylinder, four-stroke, water-cooled, naturally-aspirated, DI diesel engine	Single-cylinder, four-stroke, air-cooled, naturally-aspirated, DI diesel engine	Single-cylinder, four-stroke, air-cooled, naturally-aspirated, DI diesel engine	Single-cylinder, four-stroke, water-cooled, naturally-aspirated, DI diesel engine	Single-cylinder, four-stroke, air-cooled, naturally-aspirated, DI diesel engine	Single-cylinder, four-stroke, air-cooled, naturally-aspirated, DI diesel engine	Single-cylinder, four-stroke, air-cooled, naturally-aspirated, DI diesel engine	Single-cylinder, four-stroke, water-cooled, naturally-aspirated, DI diesel engine	Single-cylinder, four-stroke, water-cooled, naturally-aspirated, DI diesel engine	Single-cylinder, four-stroke, water-cooled, naturally-aspirated, DI diesel engine	Four-cylinder in line, four-stroke, water-cooled, naturally-aspirated, DI diesel engine	Single-cylinder, four-stroke, water-cooled, naturally-aspirated, DI diesel engine
Test conditions	– Various engine loads of 25%, 50%, 75%, and 100%	– Various engine loads of 3.75, 7.5, 11.25, 15, and 18.75 Nm	– Various engine loads of 25%, 50%, 75%, and 100%	– Various engine loads of 0, 0.87, 1.76, 2.63, and 3.5 kW	– Various engine loads of 2.5, 5, 7.5, and 10 Nm	– No load and full load	– Various engine loads of 3.75, 7.5, 11.25, 15, and 18.75 Nm	– Various engine loads of 25%, 50%, 75%, and 100%	– Various engine loads of 25%, 50%, 75%, and 100%	– Various engine loads of 25%, 50%, 75%, and 100%	– Various engine speeds of 1200, 1500, 1800, 2100, 2400, and 2600 rpm with varying loads (up to 6.8 bar brake mean effective pressure)	– Various engine loads (up to 5.81 kW)
	– At constant engine speed of 1500 rpm	– At maximum brake torque speed of 2200 rpm	– At constant engine speed of 2200 rpm	– At constant engine speed of 1500 rpm	– At constant engine speed of 1500 rpm	– Various engine speeds from 2000 to 3000 rpm	– At maximum brake torque speed of 2200 rpm	– At constant engine speed of 1500 rpm	– At constant engine speed of 1500 rpm	– At constant engine speed of 1500 rpm		– At constant engine speed of 1500 rpm
BTE	↓	↓ (Indicated thermal efficiency)	↓ (Indicated thermal efficiency)	↑	Not available	Not available	↓ (Indicated thermal efficiency)	↓	↓	↓	Almost identical at higher loads	↓
BSFC	↑	↑	↑	↓	↑	↑ (Fuel consumption)	↑	↑	↑	↑	↑	↑
BSEC	↑	Not available	Not available	Not available	Not available	Not available	Not available	↑	Not available	Not available	Not available	Not available
EGT	↑	Not available	Not available	↓	↓	↓	Not available	Not available	↓	↑	Not available	↑
NO_X	↑	↑	↑	↑ (for NO)	Not available	↓	↑	↑	↑	↑	↑	↑
CO_2	↑	↑	↑	Not available	Not available	↑	↑	Not available	Not available	Not available	Not available	Not available
CO	↓	↓	↓	↓	Not available	↓	↓	↓	↓	↓	↓	↓
UHC	↓	Not available	Not available	↓	Not available	↓	Not available	↓	↓	↓	↓	↓
O_2	↑	Not available	Not available	Not available	Not available	Not available	Not available	Not available	Not available	Not available	Not available	Not available
Smoke opacity	↓	↓	↓	Not available	Not available	Not available	↓	↓	↑	↓	↓	↑
CP_{max}	↓	↑	↑	↑ at higher loads	↑	Not available	↓	↓	↓	↓	↓	↓
PRR_{max}	Almost similar	Not available	Not available	Not available	↓	Not available	Not available	Not available	Not available	Not available	↓	Not available
HRR_{max}	↓	↑	↑	Not available	↓	Not available	↑	↓	↓	↓	↑	↓
IDP	↑	↑	↑	Not available	↑	Not available	↑	↓	Not available	Not available	Not available	↑
CHR_{max}	↓	Not available	Not available	Not available	Not available	Not available	↑	Not available	↑	Not available	Not available	Not available

of the tested fuel specimens including different biodiesel fuels as an alternating and oxygenated fuel additive or neat form in the diesel engines have been studied by various researchers. On the other hand, some of the related researches could be taken into account for the comparative analyses. Similar to the previously performed investigations, the current work figured out that the hemp seed oil methyl ester blends usage in the compression-ignition engine has caused a boost of the CO_2 emission whereas reduce the CO and UHC emissions due to the presence of the oxygen molecule in the molecular structure of the biodiesel, resulting in more complete combustion reaction inside the cylinder. However, another emission portrays a substantial variation that has been observed in the specifications of the tested engine. By all means, the remarkable enhancement was monitored in the emissions of NO_X when the engine was fueled with hemp seed oil biodiesel and its blends. This behavior has been also determined by most of the researchers. Moreover, the characteristics of the combustion were achieved similar to findings presented by different authors. To conclude, the outcomes have demonstrated the compatibility of the hemp seed oil as an alternating fuel as well as an oxygenated fuel additive to the diesel fuel for compression-ignition engine applications without any major alteration on the engine. Besides that, it can be understood that a lot of scrutinizations have to be conducted by researchers before accepting the hemp seed oil methyl ester as a direct utilization or a partial substitution for the diesel engines through the agency of the appropriate technology advance regarding the continuous harvesting of hemp plant by farmers, obtaining its crude oil, production of methyl ester, handling, storage, and other interrelated topics.

7 Conclusion

In this experimental study, biodiesel was produced by the transesterification method from the oil of industrial-grade hemp seeds, which has strategic importance as of today for most countries because it has also been supported by the state. B5, B10, B20 and B100 were obtained by blending biodiesel with diesel fuel in various proportions. A detailed analysis of the effects of all fuels on combustion, emission, and engine performance properties has been presented. The tests were implemented at different engine loads and constant engine speed. Combustion and injection characteristics, harmful pollutant characteristics, and performance characteristics were investigated. The findings obtained in the light of this study are presented stepwise as follows:

- Because the FFA value of industrial-grade hemp seed oil has less than 2%, biodiesel production was carried out by a single-stage transesterification process.
- When examining the BTE results at full load, B100 and binary fuel blends showed fewer results compared to conventional diesel fuel. The BTE values of the binary blends were 4.85%, 8.61%, and 9.85% lower than diesel fuel and 13.74%, 9.25%, and 7.77% higher than the B100, respectively. B100 caused a reduction in BTE as it somewhat reduced the energy content of the blend sample.
- It was observed that the lower calorific value of B100 fuel, which is 11.66% less than the reference diesel fuel, has reducing effects on BSFC and BSEC.
- The maximum EGTs were found to be 439.7 °C for diesel fuel, 442.5 °C for B5, 444.0 °C for B10, 451.8 °C for B20, and 454.6 °C for B100.
- The average CO emissions of B5, B10, and B20 were 11.38%, 22.97%, and 34.98% lower than diesel fuel, respectively. This is due to the influence of the natural oxygen content of the fuel mixtures tested. As a result of the usage of biodiesel blends in the diesel engine, the CO emissions quite decreased.
- When UHC outcomes were evaluated, the biodiesel blends decreased UHC emission from 0.82 g/kW h to 0.10 g/kW h. Because the UHC emission is the major contributor to photochemical smog and ozone pollution, the aforementioned reduction is very significant.
- CO_2 emission increased depending on the increase in the biodiesel ratio (approximately 61.5%), however, the released CO_2 is being absorbed by plants. For that reason, this case can be ignored when the engine is fueled with plant-based biodiesel and its blends.
- The utilization of biodiesel blends in the CI engine resulted in a more complete combustion process inside the cylinder because of their oxygen concentration chemical bonds.

In conclusion, in all the results of the present experimental study, both hemp seed oil biodiesel and its blends with diesel fuel can be evaluated for CI engine applications without any modification to the engine. It can be concluded that biodiesel can be an effective oxygen additive due to the many important benefits mentioned above. However, these tested fuel mixtures should be tested under various engine operating conditions in further experiments. In subsequent study will focus on thermodynamic, economic, and environmental analysis with the data to be obtained from industrial hemp seeds biodiesel, and diesel fuel and their blends. Increasing the interest in hemp and the necessity of blending hemp-based biodiesel fuel will increase the demand for this plant and decrease the costs. In particular, governments need to take steps in this regard. With the regulations to be made shortly, the production costs of hemp oil biodiesel can be reduced and it can become competitive with diesel fuel. However, it is clear that more research is needed on this subject. With this and similar studies, it can be thought that the interest in cannabis will increase.

Supplementary Materials

The supplementary materials of this article are available at https://stet-review.org/10.2516/stet/2022011/olm and the following is the supplementary data related to this article.

Section A: Figures

- *Figure 1S*: Hemp (*Cannabis sativa* L.) plant (This picture was taken from a trial field of Yozgat Bozok University).
- *Figure 2S*: Distribution of the hemp plant growing places in the world and Turkey.

- *Figure 3S*: The mechanism of the transesterification reaction [73].
- *Figure 4S*: Photographic views of (a) phase separation and (b) washing process.
- *Figure 5S*: Tested fuel samples used in the engine trials (from left to right: B100, diesel fuel, B5, B10, and B20).
- *Figure 6S*: A photographic view of test engine and related pieces of equipment layout.

Section B: Tables

- *Table 1S*: The test fuels using in this study along with blending ratios.
- *Table 2S*: The detailed engine specifications used in this work.
- *Table 3S*: Details of the engine instrumentations.
- *Table 4S*: The technical specifications of five gas analyzer device and smoke meter used in this work.

Acknowledgments. The authors appreciate the support supplied by the Department of Mechanical Engineering, Yozgat Bozok University, Yozgat, Turkey and Department of Automotive Technology, Kırıkkale University, Kırıkkale, Turkey for carrying out this research work. In addition, the authors would like to thank the Editors and anonymous reviewers for helping us to present a balanced account of our paper.

Availability of data

The data that support the findings of this study are available from the authors upon reasonable request.

Section of the compliance with ethical standards

Ethical approval

The authors declared that no animal and human studies are presented in this manuscript and no potentially identifiable human images or data are given in this research.

Competing interest

The authors declared that there is no competing financial interest in this research.

Conflict of interest

The authors pointed out that there is no potential conflict of interest.

Consent to participate

Not applicable.

Consent to publish

Not applicable.

Funding

This study was financially supported by the Project Coordination Application and Research Center-Scientific Research Projects Unit of Yozgat Bozok University, Yozgat, Turkey under the project number of 6602c-FBE/19-343.

CRediT authorship contribution statement

Zeki YILBAŞI: Investigation, Methodology, Data curation, Formal analysis, Visualization, Resources, Writing - original draft, Writing - review & editing.
Murat Kadir YESILYURT: Conceptualization, Investigation, Methodology, Data curation, Validation, Resources, Formal analysis, Visualization, Funding acquisition, Writing - original draft, Writing - review & editing.
Hayri YAMAN: Investigation, Methodology, Data curation, Validation, Formal analysis, Writing - review & editing.
Mevlut ARSLAN: Conceptualization, Investigation, Methodology, Data curation, Resources, Visualization, Funding acquisition, Writing – review & editing.

References

1 Ağbulut Ü., Ayyıldız M., Sarıdemir S. (2020) Prediction of performance, combustion and emission characteristics for a CI engine at varying injection pressures, *Energy* **197**, 117257.
2 Sarıkoç S., Örs İ., Ünalan S. (2020) An experimental study on energy-exergy analysis and sustainability index in a diesel engine with direct injection diesel-biodiesel-butanol fuel blends, *fuel* **268**, 117321.
3 Sarıdemir S., Ağbulut Ü. (2019) Combustion, performance, vibration and noise characteristics of cottonseed methyl ester–diesel blends fuelled engine, *Biofuels* **13**, 2, 201–210.
4 Habibullah M., Masjuki H.H., Kalam M.A., Rahman S.A., Mofijur M., Mobarak H.M., Ashraful A.M. (2015) Potential of biodiesel as a renewable energy source in Bangladesh, *Renew. Sust. Energ. Rev.* **50**, 819–834.
5 Ağbulut U. (2019) Turkey's electricity generation problem and nuclear energy policy, *Energ. Source Part A* **41**, 18, 2281–2298.
6 Ağbulut Ü., Sarıdemir S., Albayrak S. (2019) Experimental investigation of combustion, performance and emission characteristics of a diesel engine fuelled with diesel–biodiesel–alcohol blends, *J. Braz. Soc. Mech. Sci. Eng.* **41**, 9, 1–12.
7 Kumar S., Dinesha P., Rosen M.A. (2019) Effect of injection pressure on the combustion, performance and emission characteristics of a biodiesel engine with cerium oxide nanoparticle additive, *Energy* **185**, 1163–1173.
8 Uyumaz A. (2018) Combustion, performance and emission characteristics of a DI diesel engine fueled with mustard oil biodiesel fuel blends at different engine loads, *Fuel* **212**, 256–267.

9 Ağbulut Ü., Karagöz M., Sarıdemir S., Öztürk A. (2020) Impact of various metal-oxide based nanoparticles and biodiesel blends on the combustion, performance, emission, vibration and noise characteristics of a CI engine, *Fuel* **270**, 117521.

10 Kalam M.A., Masjuki H.H., Jayed M.H., Liaquat A.M. (2011) Emission and performance characteristics of an indirect ignition diesel engine fuelled with waste cooking oil, *Energy* **36**, 1, 397–402.

11 Viswanathan K., Ashok B., Pugazhendhi A. (2020) Comprehensive study of engine characteristics of novel biodiesel from curry leaf (*Murraya koenigii*) oil in ceramic layered diesel engine, *Fuel* **280**, 118586.

12 Ashok B., Nanthagopal K., Chyuan O.H., Le P.T.K., Khanolkar K., Raje N., Raj A., Karthickeyand V., Tamilvanan A. (2020) Multi-functional fuel additive as a combustion catalyst for diesel and biodiesel in CI engine characteristics, *Fuel* **278**, 118250.

13 Tamilvanan A., Balamurugan K., Ashok B., Selvakumar P., Dhamotharan S., Bharathiraja M., Karthickeyan V. (2020) Effect of diethyl ether and ethanol as an oxygenated additive on *Calophyllum inophyllum* biodiesel in CI engine, *Environ. Sci. Pollut. Res.* **28**, 33880–33898.

14 Karthickeyan V., Ashok B., Thiyagarajan S., Nanthagopal K., Geo V.E., Dhinesh B. (2019) Comparative analysis on the influence of antioxidants role with *Pistacia khinjuk* oil biodiesel to reduce emission in diesel engine, *Heat Mass Transf.* **56**, 1275–1292.

15 Ong H.C., Chen W.H., Singh Y., Gan Y.Y., Chen C.Y., Show P.L. (2020) A state-of-the-art review on thermochemical conversion of biomass for biofuel production: A TG-FTIR approach, *Energy Convers. Manag.* **209**, 112634.

16 Goh B.H.H., Ong H.C., Cheah M.Y., Chen W.H., Yu K.L., Mahlia T.M.I. (2019) Sustainability of direct biodiesel synthesis from microalgae biomass: A critical review, *Renew. Sust. Energ. Rev.* **107**, 59–74.

17 Vellaiyan S. (2020) Combustion, performance and emission evaluation of a diesel engine fueled with soybean biodiesel and its water blends, *Energy* **201**, 117633.

18 Bedir Ö., Doğan T.H. (2021) Comparison of catalytic activities of Ca-based catalysts from waste in biodiesel production, *Energ. Source Part A* 1–18.

19 Atadashi I.M., Aroua M.K., Aziz A.A., Sulaiman N.M.N. (2013) The effects of catalysts in biodiesel production: A review, *J. Ind. Eng. Chem.* **19**, 1, 14–26.

20 Verma P., Sharma M.P., Dwivedi G. (2016) Impact of alcohol on biodiesel production and properties, *Renew. Sust. Energ. Rev.* **56**, 319–333.

21 Živković S., Veljković M. (2018) Environmental impacts the of production and use of biodiesel, *Environ. Sci. Pollut. Res.* **25**, 1, 191–199.

22 Rajasekar E., Selvi S. (2014) Review of combustion characteristics of CI engines fueled with biodiesel, *Renew. Sust. Energ. Rev.* **35**, 390–399.

23 Çaynak S., Gürü M., Biçer A., Keskin A., Içingür Y. (2009) Biodiesel production from pomace oil and improvement of its properties with synthetic manganese additive, *Fuel* **88**, 3, 534–538.

24 Agarwal A.K. (2007) Biofuels (alcohols and biodiesel) applications as fuels for internal combustion engines, *Prog. Energy Combust. Sci.* **33**, 3, 233–271.

25 Canakci M., Erdil A., Arcaklioğlu E. (2006) Performance and exhaust emissions of a biodiesel engine, *Appl. Energy* **83**, 6, 594–605.

26 Mishra S., Anand K., Mehta P.S. (2016) Predicting the cetane number of biodiesel fuels from their fatty acid methyl ester composition, *Energ. Fuels* **30**, 12, 10425–10434.

27 Gharehghani A., Mirsalim M., Hosseini R. (2017) Effects of waste fish oil biodiesel on diesel engine combustion characteristics and emission, *Renew. Energy* **101**, 930–936.

28 Najafi G. (2018) Diesel engine combustion characteristics using nano-particles in biodiesel-diesel blends, *Fuel* **212**, 668–678.

29 Radhakrishnan S., Munuswamy D.B., Devarajan Y., Mahalingam A. (2019) Performance, emission and combustion study on neat biodiesel and water blends fuelled research diesel engine, *Heat Mass Transf.* **55**, 4, 1229–1237.

30 Park S.H., Kim H.J., Suh H.K., Lee C.S. (2009) Experimental and numerical analysis of spray-atomization characteristics of biodiesel fuel in various fuel and ambient temperatures conditions, *Int. J. Heat Fluid Flow* **30**, 5, 960–970.

31 Alptekin E., Canakci M. (2008) Determination of the density and the viscosities of biodiesel–diesel fuel blends, *Renew. Energy* **33**, 12, 2623–2630.

32 Ağbulut Ü., Gürel A.E., Sarıdemir S. (2021) Experimental investigation and prediction of performance and emission responses of a CI engine fuelled with different metal-oxide based nanoparticles–diesel blends using different machine learning algorithms, *Energy* **215**, 119076.

33 Jain S. (2019) The production of biodiesel using Karanja (*Pongamia pinnata*) and Jatropha (*Jatropha curcas*) Oil, in: *Biomass, Biopolymer-Based Materials, and Bioenergy*, Woodhead Publishing, pp. 397–408.

34 Arumugam A., Ponnusami V. (2019) Biodiesel production from *Calophyllum inophyllum* oil a potential non-edible feedstock: An overview, *Renew. Energy.* **131**, 459–471.

35 Hasni K., Ilham Z., Dharma S., Varman M. (2017) Optimization of biodiesel production from Brucea javanica seeds oil as novel non-edible feedstock using response surface methodology, *Energy Convers. Manag.* **149**, 392–400.

36 Muthukumaran C., Praniesh R., Navamani P., Swathi R., Sharmila G., Kumar N.M. (2017) Process optimization and kinetic modeling of biodiesel production using non-edible *Madhuca indica* oil, *Fuel* **195**, 217–225.

37 Munir M., Ahmad M., Rehan M., Saeed M., Lam S.S., Nizami A.S., Waseem A., Sultana S., Zafar M. (2021) Production of high quality biodiesel from novel non-edible *Raphnus raphanistrum* L. seed oil using copper modified montmorillonite clay catalyst, *Environ. Res.* **193**, 110398.

38 Fadhil A.B., Saleh L.A., Altamer D.H. (2020) Production of biodiesel from non-edible oil, wild mustard (*Brassica Juncea* L.) seed oil through cleaner routes, *Energ. Source Part A* **42**, 15, 1831–1843.

39 Yesilyurt M.K., Cesur C. (2020) Biodiesel synthesis from *Styrax officinalis* L. seed oil as a novel and potential non-edible feedstock: A parametric optimization study through the Taguchi technique, *Fuel* **265**, 117025.

40 Stamenković O.S., Djalović I.G., Kostić M.D., Mitrović P. M., Veljković V.B. (2018) Optimization and kinetic modeling of oil extraction from white mustard (*Sinapis alba* L.) seeds, *Ind. Crops Prod.* **121**, 132–141.

41 Aslan V., Eryilmaz T. (2020) Polynomial regression method for optimization of biodiesel production from black mustard (*Brassica nigra* L.) seed oil using methanol, ethanol, NaOH, and KOH, *Energy* **209**, 118386.

42 Onoji S.E., Iyuke S.E., Igbafe A.I., Daramola M.O. (2020) Rubber seed (*Hevea brasiliensis*) oil biodiesel emission profiles and engine performance characteristics using a TD202 diesel test engine, *Biofuels* **13**, 4, 423–430.

43 Uyaroğlu A., Uyumaz A., Çelikten İ. (2018) Comparison of the combustion, performance, and emission characteristics of inedible *Crambe abyssinica* biodiesel and edible hazelnut, corn, soybean, sunflower, and canola biodiesels, *Environ. Prog. Sustain. Energy* **37**, 4, 1438–1447.

44 Ahmad M., Ullah K., Khan M.A., Zafar M., Tariq M., Ali S., Sultana S. (2011) Physicochemical analysis of hemp oil biodiesel: a promising non edible new source for bioenergy, *Energ. Source Part A* **33**, 14, 1365–1374.

45 John C.B., Raja S.A. (2020) Analysis of combustion, emission and performance attributes of hemp biodiesel on a compression ignition engine, *World Rev. Sci. Technol. Sustain. Dev.* **16**, 2, 169–183.

46 Mohammed M.N., Atabani A.E., Uguz G., Lay C.H., Kumar G., Al-Samaraae R.R. (2020) Characterization of hemp (*Cannabis sativa* L.) biodiesel blends with euro diesel, butanol and diethyl ether using FT-IR, UV-Vis, TGA and DSC techniques, *Waste Biomass Valorize* **11**, 3, 1097–1113.

47 Li S.Y., Stuart J.D., Li Y., Parnas R.S. (2010) The feasibility of converting *Cannabis sativa* L. oil into biodiesel, *Bioresource Technol.* **101**, 21, 8457–8460.

48 Gupta A.R., Jalan A.P., Rathod V.K. (2018) Solar energy as a process intensification tool for the biodiesel production from hempseed oil, *Energy Convers. Manag.* **171**, 126–132.

49 Stamenković O.S., Veličković A.V., Kostić M.D., Joković N. M., Rajković K.M., Milić P.S., Veljković V.B. (2015) Optimization of KOH-catalyzed methanolysis of hempseed oil, *Energy Convers. Manag.* **103**, 235–243.

50 Ravichandra D., Puli R.K., Chandramohan V.P., Geo V.E. (2019) Experimental analysis of Deccan hemp oil as a new energy feedstock for compression ignition engine, *Int. J. Ambient. Energy* **40**, 6, 634–644.

51 Jayaraman K., Babu G.N., Dhandapani G., Varuvel E.G. (2019) Effect of hydrogen addition on performance, emission, and combustion characteristics of Deccan hemp oil and its methyl ester–fuelled CI engine, *Environ. Sci. Pollut. Res.* **26**, 9, 8685–8695.

52 USDA (2020) *Plant database, natural resources conservation service*. Available at: https://plants.sc.egov.usda.gov/core/profile?symbol=CASA3 [Access Date: 04.03.2021].

53 Ragit S.S., Mohapatra S.K., Gill P., Kundu K. (2012) Brown hemp methyl ester: transesterification process and evaluation of fuel properties, *Biomass and Bioenerg.* **41**, 14–20.

54 Ur Rehman M.S., Rashid N., Saif A., Mahmood T., Han J.-I. (2013) Potential of bioenergy production from industrial hemp (Cannabis sativa): Pakistan perspective, *Renew. Sust. Energ. Rev.* **18**, 154–164.

55 Johnson R. (2014) *Hemp as an agricultural commodity*, Library of Congress Washington DC Congressional Research Service, pp. 48.

56 Kiralan M., Gül V., Kara S.M. (2010) Fatty acid composition of hempseed oils from different locations in Turkey, *Span. J. Agric. Res.* **2**, 385–390.

57 Milano J., Ong H.C., Masjuki H.H., Silitonga A.S., Chen W.H., Kusumo F., Drahma S., Sebayang A.H. (2018) Optimization of biodiesel production by microwave irradiation-assisted transesterification for waste cooking oil-*Calophyllum inophyllum* oil *via* response surface methodology, *Energy Convers, Manag.* **158**, 400–415.

58 Asokan M.A., Kamesh S., Khan W. (2018) Performance, combustion and emission characteristics of diesel engine fuelled with papaya and watermelon seed oil biodiesel/diesel blends, *Energy* **145**, 238–245.

59 Silitonga A.S., Mahlia T.M.I., Ong H.C., Riayatsyah T.M. I., Kusumo F., Ibrahim H., Drahma S., Gumilang D. (2017) A comparative study of biodiesel production methods for *Reutealis trisperma* biodiesel, *Energ. Source Part A* **39**, 20, 2006–2014.

60 Prabu S.S., Asokan M.A., Prathiba S., Ahmed S., Puthean G. (2018) Effect of additives on performance, combustion and emission behavior of preheated palm oil/diesel blends in DI diesel engine, *Renew. Energy* **122**, 196–205.

61 Eryilmaz T., Yesilyurt M.K. (2016) Influence of blending ratio on the physicochemical properties of safflower oil methyl ester-safflower oil, safflower oil methyl ester-diesel and safflower oil-diesel, *Renew. Energy* **95**, 233–247.

62 Asokan M.A., Prabu S.S., Bade P.K.K., Nekkanti V.M., Gutta S.S.G. (2019) Performance, combustion and emission characteristics of juliflora biodiesel fuelled DI diesel engine, *Energy* **173**, 883–892.

63 Uyumaz A. (2020) Experimental evaluation of linseed oil biodiesel/diesel fuel blends on combustion, performance and emission characteristics in a DI diesel engine, *Fuel* **267**, 117150.

64 Venkanna B.K., Reddy C.V. (2009) Biodiesel production and optimization from *Calophyllum inophyllum* linn oil (honne oil) – A three stage method, *Bioresource Technol.* **100**, 21, 5122–5125.

65 Ramadhas A.S., Jayaraj S., Muraleedharan C. (2005) Biodiesel production from high FFA rubber seed oil, *Fuel* **84**, 4, 335–340.

66 Prabu S.S., Asokan M.A., Roy R., Francis S., Sreelekh M.K. (2017) Performance, combustion and emission characteristics of diesel engine fuelled with waste cooking oil biodiesel/diesel blends with additives, *Energy* **122**, 638–648.

67 Ramadhas A.S., Jayaraj S., Muraleedharan C. (2005) Characterization and effect of using rubber seed oil as fuel in the compression ignition engines, *Renew. Energy* **30**, 5, 795–803.

68 How H.G., Masjuki H.H., Kalam M.A., Teoh Y.H. (2014) An investigation of the engine performance, emissions and combustion characteristics of coconut biodiesel in a high-pressure common-rail diesel engine, *Energy* **69**, 749–759.

69 Doğan B., Erol D., Yaman H., Kodanli E. (2017) The effect of ethanol-gasoline blends on performance and exhaust emissions of a spark ignition engine through exergy analysis, *Appl. Therm. Eng.* **120**, 433–443.

70 Emiroğlu A.O., Şen M. (2018) Combustion, performance and exhaust emission characterizations of a diesel engine operating with a ternary blend (alcohol-biodiesel-diesel fuel), *Appl. Therm. Eng.* **133**, 371–380.

71 Erdoğan S., Balki M.K., Sayin C. (2019) The effect on the knock intensity of high viscosity biodiesel use in a DI diesel engine, *Fuel* **253**, 1162–1167.

72 Heywood J.B. (2018) *Internal combustion engine fundamentals*, McGraw-Hill Education.

73 Debnath B.K., Bora B.J., Sahoo N., Saha U.K. (2014) Influence of emulsified palm biodiesel as pilot fuel in a biogas run dual fuel diesel engine, *J. Energ. Eng.* **140**, 3, A4014005.

74 Bora B.J., Saha U.K. (2016) Experimental evaluation of a rice bran biodiesel–biogas run dual fuel diesel engine at varying compression ratios, *Renew. Energy* **87**, 782–790.

75 Bora B.J., Saha U.K., Chatterjee S., Veer V. (2014) Effect of compression ratio on performance, combustion and emission characteristics of a dual fuel diesel engine run on raw biogas, *Energy Convers. Manag.* **87**, 1000–1009.

76 Erdoğan S., Balki M.K., Sayin C. (2019) Combustion analysis of biodiesel derived from bone marrow in a diesel generator at low loads, *Int. J. Automot. Technol.* **8**, 2, 76–82.

77 Soloiu V., Gaubert R., Moncada J., Wiley J., Williams J., Harp S., Ilie M., Molina G., Mothershed D. (2019) Reactivity controlled compression ignition and low temperature combustion of Fischer-Tropsch fuel blended with n-butanol, *Renew. Energy* **134**, 1173–1189.

78 Soloiu V., Moncada J.D., Gaubert R., Knowles A., Molina G., Ilie M., Harp S., Wiley J.T. (2018) Reactivity controlled compression ignition combustion and emissions using n-butanol and methyl oleate, *Energy* **165**, 911–924.

79 Wei L., Yao C., Han G., Pan W. (2016) Effects of methanol to diesel ratio and diesel injection timing on combustion, performance and emissions of a methanol port premixed diesel engine, *Energy* **95**, 223–232.

80 Vavra J., Bohac S.V., Manofsky L., Lavoie G., Assanis D. (2012) Knock in various combustion modes in a gasoline-fueled automotive engine, *J. Eng. Gas. Turbine Power* **134**, 8.

81 Merker G.P., Schwarz C., Teichmann R., (eds), (2011) *Combustion engines development: mixture formation, combustion, emissions and simulation*, Springer Science & Business Media.

82 Holman P. (2012) *Experimental methods for engineers*, 8th edn., McGraw-Hill, New York, USA.

83 Rajak U., Nashine P., Verma T.N. (2020) Effect of spirulina microalgae biodiesel enriched with diesel fuel on performance and emission characteristics of CI engine, *Fuel* **268**, 117305.

84 Shrivastava P., Verma T.N., Pugazhendhi A. (2019) An experimental evaluation of engine performance and emisssion characteristics of CI engine operated with Roselle and Karanja biodiesel, *Fuel* **254**, 115652.

85 Rajak U., Verma T.N. (2018) Effect of emission from ethylic biodiesel of edible and non-edible vegetable oil, animal fats, waste oil and alcohol in CI engine, *Energy Convers. Manag.* **166**, 704–718.

86 Dhar A., Agarwal A.K. (2014) Performance, emissions and combustion characteristics of Karanja biodiesel in a transportation engine, *Fuel* **119**, 70–80.

87 Chauhan B.S., Kumar N., Cho H.M. (2012) A study on the performance and emission of a diesel engine fueled with Jatropha biodiesel oil and its blends, *Energy* **37**, 1, 616–622.

88 Qi D.H., Chen H., Geng L.M., Bian Y.Z. (2010) Experimental studies on the combustion characteristics and performance of a direct injection engine fueled with biodiesel/diesel blends, *Energy Convers. Manag.* **51**, 12, 2985–2992.

89 Vedharaj S., Vallinayagam R., Yang W.M., Chou S.K., Chua K.J.E., Lee P.S. (2013) Experimental investigation of kapok (Ceiba pentandra) oil biodiesel as an alternate fuel for diesel engine, *Energy Convers. Manag.* **75**, 773–779.

90 Agarwal A.K., Dhar A. (2013) Experimental investigations of performance, emission and combustion characteristics of Karanja oil blends fuelled DICI engine, *Renew. Energy* **52**, 283–291.

91 Shrivastava P., Verma T.N. (2020) Effect of fuel injection pressure on the characteristics of CI engine fuelled with biodiesel from Roselle oil, *Fuel* **265**, 117005.

92 Rajak U., Verma T.N. (2020) Influence of combustion and emission characteristics on a compression ignition engine from a different generation of biodiesel, *Eng. Sci. Technol. Int. J.* **23**, 1, 10–20.

93 Karmee S.K., Chadha A. (2005) Preparation of biodiesel from crude oil of *Pongamia pinnata*, *Bioresource Technol.* **96**, 13, 1425–1429.

94 Lakshmi Narayana Rao G., Durga Prasad B., Sampath S., Rajagopal K. (2007) Combustion analysis of diesel engine fueled with jatropha oil methyl ester-diesel blends, *Int. J. Green Energy* **4**, 6, 645–658.

95 Hoekman S.K., Robbins C. (2012) Review of the effects of biodiesel on NOx emissions, *Fuel Process. Technol.* **96**, 237–249.

96 Deepanraj B., Sankaranarayanan G., Senthilkumar N., Pugazhvadivu M. (2017) Influence of dimethoxymethane addition on performance, emission and combustion characteristics of the diesel engine, *Int. J. Ambient. Energy* **38**, 6, 622–626.

97 Rajak U., Verma T.N. (2019) A comparative analysis of engine characteristics from various biodiesels: Numerical study, *Energy Convers. Manag.* **180**, 904–923.

98 Dhinesh B., Lalvani J.I.J., Parthasarathy M., Annamalai K. (2016) An assessment on performance, emission and combustion characteristics of single cylinder diesel engine powered by *Cymbopogon flexuosus* biofuel, *Energy Convers. Manag.* **117**, 466–474.

99 Abedin M.J., Kalam M.A., Masjuki H.H., Sabri M.F.M., Rahman S.A., Sanjid A., Fattah I.R. (2016) Production of biodiesel from a non-edible source and study of its combustion, and emission characteristics: A comparative study with B5, *Renew. Energy* **88**, 20–29.

100 Bayındır H., Işık M.Z., Argunhan Z., Yücel H.L., Aydın H. (2017) Combustion, performance and emissions of a diesel power generator fueled with biodiesel-kerosene and biodiesel-kerosene-diesel blends, *Energy* **123**, 241–251.

101 Ramesh A., Ashok B., Nanthagopal K., Pathy M.R., Tambare A., Mali P., Phuke P., Patil S., Subbarao R. (2019) Influence of hexanol as additive with *Calophyllum Inophyllum* biodiesel for CI engine applications, *Fuel* **249**, 472–485.

102 Maurya R.K., Saxena M.R. (2018) Characterization of ringing intensity in a hydrogen-fueled HCCI engine, *Int. J. Hydrog. Energy* **43**, 19, 9423–9437.

103 Eng J.A. (2002) *Characterization of pressure waves in HCCI combustion*, (No. 2002-01-2859), SAE Technical Paper.

104 Uludamar E., Tosun E., Aydın K. (2016) Experimental and regression analysis of noise and vibration of a compression ignition engine fuelled with various biodiesels, *Fuel* **177**, 326–333.

105 Yesilyurt M.K. (2020) A detailed investigation on the performance, combustion, and exhaust emission characteristics of a diesel engine running on the blend of diesel fuel, biodiesel and 1-heptanol (C7 alcohol) as a next-generation higher alcohol, *Fuel* **275**, 117893.

106 Soloiu V., Knowles A., Moncada J., Simons E., Muinos M., Beyerl T. (2017) *Investigations on gaseous emissions, sound and vibrations levels of a DI engine fueled with 100% cottonseed biodiesel (No. 2017-01-0700)*, SAE Technical Paper.

107 Özgür T. (2019) Performance, emission, energetic and exergetic analyses of a compression ignition engine fuelled with sunflower oil methyl esters, *Int. J. Automot. Technol.* **8**, 2, 70–75.

108 Koç M., Sekmen Y., Topgül T., Yücesu H.S. (2009) The effects of ethanol–unleaded gasoline blends on engine performance and exhaust emissions in a spark-ignition engine, *Renew. Energy* **34**, 10, 2101–2106.

109 Varol Y., Öner C., Öztop H.F., Altun Ş. (2014) Comparison of methanol, ethanol, or n-butanol blending with unleaded gasoline on exhaust emissions of an SI engine, *Energ. Source Part A* **36**, 9, 938–948.

110 Damanik N., Ong H.C., Tong C.W., Mahlia T.M.I., Silitonga A.S. (2018) A review on the engine performance and exhaust emission characteristics of diesel engines fueled with biodiesel blends, *Environ. Sci. Pollut. Res.* **25**, 16, 15307–15325.

111 Silitonga A.S., Masjuki H.H., Ong H.C., Sebayang A.H., Dharma S., Kusumo F., Siswantoro J., Milano J., Daud K., Mahlia T.M.I., Wei-Hsin Chen, Sugiyanto B. (2018) Evaluation of the engine performance and exhaust emissions of biodiesel-bioethanol-diesel blends using kernel-based extreme learning machine, *Energy* **159**, 1075–1087.

112 Masum B.M., Masjuki H.H., Kalam M.A., Palash S.M., Wakil M.A., Imtenan S. (2014) Tailoring the key fuel properties using different alcohols (C2–C6) and their evaluation in gasoline engine, *Energy Convers. Manag.* **88**, 382–390.

113 Zaharin M.S.M., Abdullah N.R., Masjuki H.H., Ali O.M., Najafi G., Yusaf T. (2018) Evaluation on physicochemical properties of iso-butanol additives in ethanol-gasoline blend on performance and emission characteristics of a spark-ignition engine, *Appl. Therm. Eng.* **144**, 960–971.

114 Gupta H.N. (2012) *Fundamentals of internal combustion engines*, PHI Learning Pvt., Ltd.

115 Özener O., Yüksek L., Ergenç A.T., Özkan M. (2014) Effects of soybean biodiesel on a DI diesel engine performance, emission and combustion characteristics, *Fuel* **115**, 875–883.

116 Nabi M.N., Rahman M.M., Akhter M.S. (2009) Biodiesel from cotton seed oil and its effect on engine performance and exhaust emissions, *Appl. Therm. Eng.* **29**, 11–12, 2265–2270.

117 Canakci M. (2005) Performance and emissions characteristics of biodiesel from soybean oil, *P. I. Mech. Eng. D-J. Aut.* **219**, 7, 915–922.

118 Aydın F., Öğüt H. (2017) Effects of using ethanol-biodiesel-diesel fuel in single cylinder diesel engine to engine performance and emissions, *Renew. Energy* **103**, 688–694.

119 Sharudin H., Abdullah N.R., Najafi G., Mamat R., Masjuki H.H. (2017) Investigation of the effects of iso-butanol additives on spark ignition engine fuelled with methanol-gasoline blends, *Appl. Therm. Eng.* **114**, 593–600.

120 Pulkrabek W.W. (1997) *Engineering fundamentals of the internal combustion engine, No. 621.43*, Pearson New International Edition, Pearson Higher Ed..

121 Enweremadu C.C., Rutto H.L. (2010) Combustion, emission and engine performance characteristics of used cooking oil biodiesel – A review, *Renew. Sust. Energ. Rev.* **14**, 9, 2863–2873.

122 Pinzi S., Rounce P., Herreros J.M., Tsolakis A., Dorado M.P. (2013) The effect of biodiesel fatty acid composition on combustion and diesel engine exhaust emissions, *Fuel* **104**, 170–182.

123 Balaji D., Govindarajan P., Venkatesan J. (2010) Emission and combustion characteristics of SI engine working under gasoline blended with ethanol oxygenated organic compounds, *Am. J. Environ. Sci.* **6**, 6, 495.

124 Sharma A., Murugan S. (2013) Investigation on the behaviour of a DI diesel engine fueled with Jatropha Methyl Ester (JME) and Tyre Pyrolysis Oil (TPO) blends, *Fuel* **108**, 699–708.

125 Mofijur M., Masjuki H.H., Kalam M.A., Atabani A.E. (2013) Evaluation of biodiesel blending, engine performance and emissions characteristics of *Jatropha curcas* methyl ester: Malaysian perspective, *Energy* **55**, 879–887.

126 Fattah I.R., Masjuki H.H., Kalam M.A., Wakil M.A., Ashraful A.M., Shahir S.A. (2014) Experimental investigation of performance and regulated emissions of a diesel engine with *Calophyllum inophyllum* biodiesel blends accompanied by oxidation inhibitors, *Energy Convers. Manag.* **83**, 232–240.

127 Ashok B., Nanthagopal K., Vignesh D.S. (2018) *Calophyllum inophyllum* methyl ester biodiesel blend as an alternate fuel for diesel engine applications, *Alex. Eng. J.* **57**, 3, 1239–1247.

128 Ashok B., Nanthagopal K., Senthil Kumar M., Ramasamy A., Patel D., Balasubramanian S., Balakrishnan S. (2019) An investigation on CI engine characteristics using pork lard methyl ester at various injection pressures and injection timings, *Int. J. Green Energy* **16**, 11, 834–846.

129 Feng R., Yang J., Zhang D., Deng B., Fu J., Liu J., Liu X. (2013) Experimental study on SI engine fuelled with butanol–gasoline blend and H_2O addition, *Energy Convers. Manag.* **74**, 192–200.

130 Silitonga A.S., Hassan M.H., Ong H.C., Kusumo F. (2017) Analysis of the performance, emission and combustion characteristics of a turbocharged diesel engine fuelled with *Jatropha curcas* biodiesel-diesel blends using kernel-based extreme learning machine, *Environ. Sci. Pollut. Res.* **24**, 32, 25383–25405.

131 Rahman S.A., Masjuki H.H., Kalam M.A., Abedin M.J., Sanjid A., Sajjad H. (2013) Production of palm and *Calophyllum inophyllum* based biodiesel and investigation of blend performance and exhaust emission in an unmodified diesel engine at high idling conditions, *Energy Convers. Manag.* **76**, 362–367.

132 Yesilyurt M.K., Eryilmaz T., Arslan M. (2018) A comparative analysis of the engine performance, exhaust emissions and combustion behaviors of a compression ignition engine fuelled with biodiesel/diesel/1-butanol (C4 alcohol) and biodiesel/diesel/n-pentanol (C5 alcohol) fuel blends, *Energy* **165**, 1332–1351.

133 Krishania N., Rajak U., Chaurasiya P.K., Singh T.S., Birru A.K., Verma T.N. (2020) Investigations of spirulina, waste cooking and animal fats blended biodiesel fuel on auto-ignition diesel engine performance, emission characteristics, *Fuel* **276**, 118123.

134 Elsanusi O.A., Roy M.M., Sidhu M.S. (2017) Experimental investigation on a diesel engine fueled by diesel-biodiesel blends and their emulsions at various engine operating conditions, *Appl. Energy* **203**, 582–593.

135 Jamuwa D.K., Sharma D., Soni S.L. (2016) Experimental investigation of performance, exhaust emission and combustion parameters of stationary compression ignition engine using ethanol fumigation in dual fuel mode, *Energy Convers. Manag.* **115**, 221–231.

136 Ong H.C., Masjuki H.H., Mahlia T.M.I., Silitonga A.S., Chong W.T., Leong K.Y. (2014) Optimization of biodiesel production and engine performance from high free fatty acid *Calophyllum inophyllum* oil in CI diesel engine, *Energy Convers. Manag.* **81**, 30–40.

137 Balusamy T., Marappan R. (2007) Performance evaluation of direct injection diesel engine with blends of *Thevetia peruviana* seed oil and diesel, *J. Sci. Ind. Res. (India)* **66**, 12, 1035–1040.
138 Kandasamy K.T., Rakkiyanna G.M. (2011) *Thevetia peruviana* biodiesel emulsion used as a fuel in a single cylinder diesel engine reduces NOx and smoke, *Thermal Sci.* **15**, 4, 1185–1191.
139 Panwar N.L., Shrirame H.Y., Rathore N.S., Jindal S., Kurchania A.K. (2010) Performance evaluation of a diesel engine fueled with methyl ester of castor seed oil, *Appl. Therm. Eng.* **30**, 2–3, 245–249.
140 Devan P.K., Mahalakshmi N.V. (2009) Study of the performance, emission and combustion characteristics of a diesel engine using poon oil-based fuels, *Fuel Process. Technol.* **90**, 4, 513–519.
141 Uyumaz A., Aydoğan B., Yılmaz E., Solmaz H., Aksoy F., Mutlu İ., İpci D., Calam A. (2020) Experimental investigation on the combustion, performance and exhaust emission characteristics of poppy oil biodiesel-diesel dual fuel combustion in a CI engine, *Fuel* **280**, 118588.
142 Das M., Sarkar M., Datta A., Santra A.K. (2018) An experimental study on the combustion, performance and emission characteristics of a diesel engine fuelled with diesel-castor oil biodiesel blends, *Renew. Energy* **119**, 174–184.
143 Tayari S., Abedi R., Tahvildari K. (2020) Experimental investigation on fuel properties and engine characteristics of biodiesel produced from *Eruca sativa*, *SN Appl. Sci.* **2**, 1, 1–13.
144 Raman L.A., Deepanraj B., Rajakumar S., Sivasubramanian V. (2019) Experimental investigation on performance, combustion and emission analysis of a direct injection diesel engine fuelled with rapeseed oil biodiesel, *Fuel* **246**, 69–74.